Journal of Medicinal Chemistry

Article

pubs.acs.org/jmc

Development of a Novel Nonpeptidic ^{18}F-Labeled Radiotracer for in Vivo Imaging of Oxytocin Receptors with Positron Emission Tomography

Barbara Wenzel,[*,†,#] Jan Mollitor,[‡,#] Winnie Deuther-Conrad,[†] Sladjana Dukic-Stefanovic,[†] Mathias Kranz,[†] Chrysoula Vraka,[§] Rodrigo Teodoro,[†] Robert Günther,[†] Cornelius K. Donat,[†] Friedrich-Alexander Ludwig,[†] Steffen Fischer,[†] Rene Smits,[‡] Wolfgang Wadsak,[§] Markus Mitterhauser,[§] Jörg Steinbach,[†] Alexander Hoepping,[‡] and Peter Brust[†]

[†]Helmholtz-Zentrum Dresden-Rossendorf, Institute of Radiopharmaceutical Cancer Research, Research Site Leipzig, Department of Neuroradiopharmaceuticals,, Permoserstr. 15, 04318 Leipzig, Germany

[‡]ABX Advanced Biochemical Compounds GmbH, 01454 Radeberg, Germany

[§]Radiopharmacy and Experimental Nuclear Medicine, Division of Nuclear Medicine, Medical University of Vienna, A-1090 Vienna, Austria

ABSTRACT: With the aim of imaging and quantification of oxytocin receptors (OTRs) in living brain using positron emission tomography (PET), we developed a ^{18}F-labeled small molecule radiotracer and investigated its in vivo pharmacokinetics in mice and pig. [^{18}F]**6b** (K_D = 12.3 nM) was radiolabeled by a two-step procedure using a microwave system with radiochemical yields of 26.9 ± 4.7%. Both organ distribution and small animal PET studies revealed limited brain uptake of [^{18}F]**6b** in mouse (mean SUV of 0.04 at 30 min pi). Besides, significant radioactivity uptake in the pituitary gland was observed (SUV of 0.7 at 30 min pi). In a dynamic PET study in one piglet, we detected a higher uptake of [^{18}F]**6b** in the olfactory bulb (SUV of 0.34 at 30 min pi) accompanied by a low uptake in the whole brain. In vitro autoradiographic studies on porcine brain sections indicated interaction of [^{18}F]**6b** with several off-target receptors.

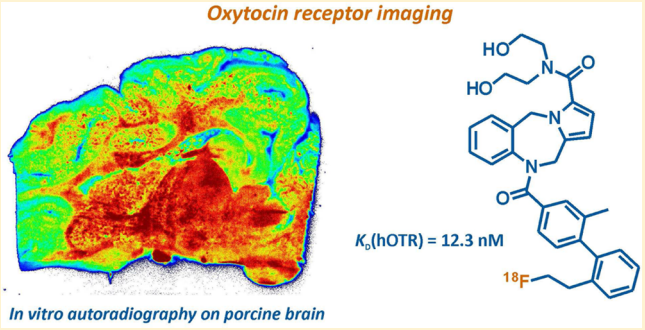

1. INTRODUCTION

The small peptide oxytocin consists of nine amino acids arranged in a disulfide-bonded cyclic structure with a short "tail". It is mainly synthesized in the paraventricular nuclei of the hypothalamus as a large prohormone, cleaved into the biologically active oxytocin and neurophysin I during passage in the neurohypophysis, and secreted upon activation of the neurosecretory cells by multiple physiological stimuli.[1] It binds to the oxytocin receptor (OTR), a 389 amino acid polypeptide (human OTR) belonging to the G-protein coupled receptor (GPCR) family. OTRs are peripherally expressed mainly in the uterus, the mammary gland, the ovary, the testis, the prostate, the kidney, the heart, and bone.[2] In the uterus, they mediate the contracting effect of oxytocin, the first discovered action of this hormone. Beside peripheral physiological functions,[2,3] oxytocin also plays an important role in the central nervous system, where it acts as putative neurotransmitter and neurohormone in different brain regions. The OTR expression in brain is strongly species-dependent,[2] which hampers the comparability between data obtained in animals and human. Main OTR expressing brain regions in human are basal ganglia, hypothalamic nuclei, brain stem, basal nucleus of Meynert, and the lateral septal nucleus.[2] Although investigated by autoradiography,[4] no quantitative data on OTR expression in human brain are available yet. A semiquantitative study on monkey brain revealed comparatively high expression in hippocampus and moderate expression in nucleus basalis of Meynert and some cortical and hindbrain regions.[5] In rats, however, beside the basal ganglia and the hypothalamus, OTRs are also abundantly expressed (~200−400 fmol [^{3}H]OT/mg protein) in the olfactory system (anterior olf nucl), the bed nucleus of stria terminalis, and the peduncular cortex.[2,6,7] In addition, Freund-Mercier et al.[8] have shown that neurophysins rather than OTR are involved in binding of [^{3}H]oxytocin in the neural lobe of the pituitary.

Central behavioral effects of the OT system are extensively investigated in animals[9−11] and in humans.[12−15] The involvement in social and maternal behavior, trust and empathy, partnership bonding, sexual behavior, stress-related behavior, and learning and memory has been demonstrated.[12,16] Moreover, the impact of oxytocin on psychiatric disorders such as schizophrenia,[17] depression,[18] and autism[19,20] is the object of recent studies. Research in this field is mainly

Received: August 18, 2015

DOI: 10.1021/acs.jmedchem.5b01080
J. Med. Chem. XXXX, XXX, XXX−XXX

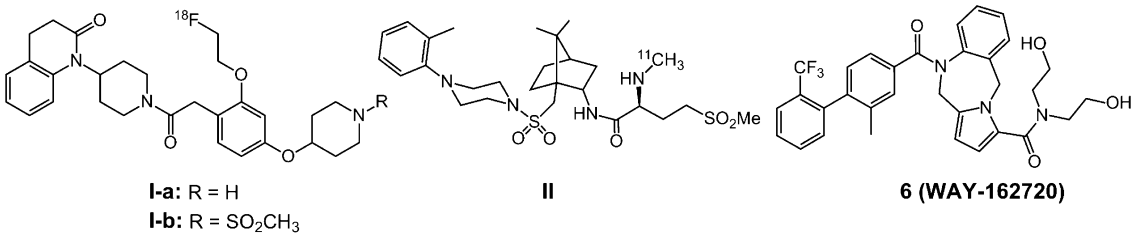

Figure 1. Reported PET radiotracers for OTR (**I-a**, **I-b**, and **II**); **6** as lead structure.

Scheme 1. Synthetic Route of Series A Derivatives 6a–6f and Precursor 7[a]

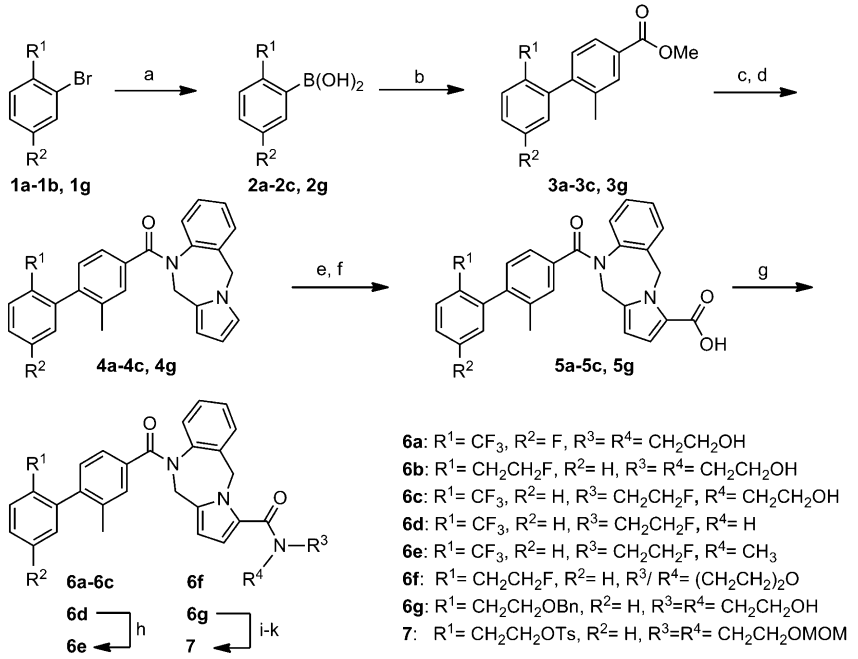

[a]Reagents and conditions: (a) $B(OMe)_3$, *n*-BuLi, THF, −78 °C to rt; (b) methyl 4-bromo-3-methylbenzoate, $Pd(PPh_3)_4$, Na_2CO_3, H_2O, EtOH, toluene, 14 h, 90 °C; (c) 1 M NaOH, THF, 12 h, reflux; (d) (i) $SOCl_2$, 2 h, reflux, (ii) 10,11-dihydro-5*H*-pyrrolo[2,1-*c*][1,4]benzodiazepine (**8**), Hünig's base, CH_2Cl_2, 0 °C to rt, overnight; (e) trichloroacetyl chloride, Hünig's base, CH_2Cl_2, 2 h, 0 °C to rt achieving intermediates **15**, **18**, and **19**; (f) 2.5 M NaOH, acetone, 12 h, rt; (g) amidation with the corresponding amine (for **6a**,**b**,**g**, diethanolamine; for **6c**, diethanolamine and DAST, CH_2Cl_2, 12 h, rt; for **6d**,**6e**, 2-fluoroethylamine; for **6f**, morpholine) HOBt/EDCI, COMU, or TBTU, 12–20 h, rt; (h) NaH, CH_3I, DMF, 1 h, rt; (i) MOMBr, TBAC, Hünig's base, CH_2Cl_2, 24 h, 0 °C to rt achieving intermediate **16**; (j) H_2, $Pd(OH)_2$/C, MeOH, 20 h, rt achieving intermediate **17**; (k) TsCl, triethylamine, 4-DMAP, CH_2Cl_2, 12 h, 0 °C to rt.

conducted by behavioral monitoring after drug administration or functional magnetic resonance imaging (fMRI), the latter based on changes in the blood flow in certain brain regions.[14] An investigation of disease-specific changes in the expression of OTR in the brain has been limited so far.

Positron emission tomography (PET) is a noninvasive imaging method that can provide selective information on a single biological target or biochemical process, when a target specific radiotracer is used. Therefore, a radiotracer, binding specifically to the OTR, would allow direct quantification of these receptors in the living brain and open new options for diagnosis and therapy monitoring of the diseases mentioned above.

In 2012 and 2013, Smith et al. reported for the first time structurally different PET tracers intended for OTR imaging (see **I-a**, **I-b**, and **II** in Figure 1), labeled with fluorine-18 and carbon-11, the most commonly used short-lived positron emitting radionuclides.[21−23] These compounds are based on two nonpeptidic antagonists of the OTR developed by Merck Research Laboratories in the early 1990s as drug candidates for premature labor.[24,25] Although these small molecule radiotracers showed appropriate physicochemical properties regarding blood–brain barrier (BBB) permeability, the authors observed a very poor brain uptake in rats and cynomolgus monkeys insufficient for OTR imaging.

In parallel to this work, we started to develop a ^{18}F-labeled PET radiotracer for imaging of OTR in brain. As lead structure, *N*,*N*-bis(2-hydroxyethyl)-10-(2-methyl-2′-(trifluoromethyl)-[1,1′-biphenyl]-4-carbonyl)-10,11-dihydro-5*H*-benzo[*e*]-pyrrolo[1,2-*a*][1,4]diazepine-3-carboxamide, **6** (**WAY-162720**;[26] Figure 1), was selected, an OTR antagonist described to be able to penetrate the BBB in mice.[27] We synthesized two series of derivatives and determined the binding affinity toward human OTR (hOTR) in vitro as well as their lipophilicity (log *D*) and permeability values (P_m) by different HPLC methods. The most promising candidate was labeled with [^{18}F]fluoride and investigated by in vitro autoradiography on pig brain slices. Furthermore, the pharmacokinetics of the novel ^{18}F-labeled PET radiotracer

DOI: 10.1021/acs.jmedchem.5b01080
J. Med. Chem. XXXX, XXX, XXX−XXX

Scheme 2. Synthetic Route of Series B Derivatives 12a−12d, 13a, 13b, and 14[a]

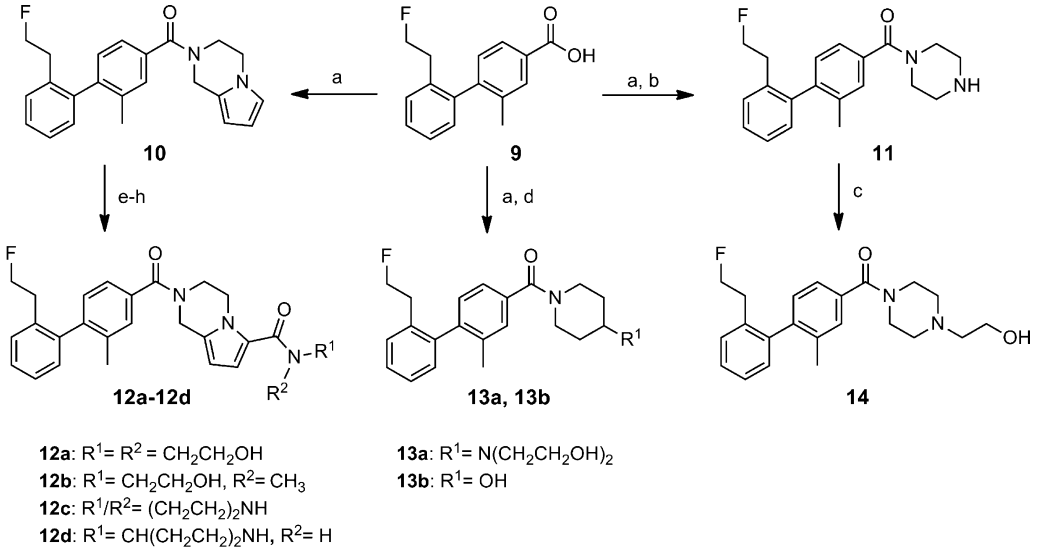

[a]Reagents and conditions: (a) (i) $SOCl_2$, 1 h, reflux; (ii) Hünig's base, CH_2Cl_2, and 1,2,3,4-tetrahydro-pyrrolo[1,2-*a*]pyrazine for **12a−d**, 4-piperidone for **13a,b**, and intermediate **24**, *N*-Boc-piperazine for **14** and intermediate **25**, 4 h, 0 °C to rt; (b) trifluoroacetic acid, CH_2Cl_2, 2.5 h, rt; (c) 2-bromoethanol, K_2CO_3, CH_3CN, 12 h, reflux; (d) diethanolamine, $Na(OAc)_3BH$, AcOH, 1,2-dichloroethane, 12 h, rt; (e) trichloroacetyl chloride, Hünig's base, CH_2Cl_2, 2 h, 0 °C to rt achieving intermediate **20**; (f) 2.5 M NaOH, acetone, 12 h, rt achieving intermediate **21**; (g) amidation with the corresponding amine (**12a**, diethanolamine; **12b**, *N*-methylethanolamine; **12c** and intermediate **22**, *N*-Boc-piperazine; **12d** and intermediate **23**, 4-amino-1-Boc-piperidine) HOBt/EDCI, COMU, or TBTU, 12−20 h, rt; (h) **12c,d**, trifluoroacetic acid, CH_2Cl_2, 2,5 h, rt.

was investigated in mice and pig by ex vivo analyses and dynamic PET studies.

2. RESULTS AND DISCUSSION

2.1. Organic Chemistry. The synthesis of the new derivatives is based on the synthesis of **6** described previously.[26] Key steps of the synthetic routes are a Suzuki coupling between appropriately substituted phenylboronic acids and methyl 4-bromo-3-methylbenzoate to form the desired biaryl framework, followed by an amidation using a tricyclic benzodiazepine (series A, Scheme 1) or other *N*-heterocycles like piperazine, piperidine, and pyrrolopyrazine (series B, Scheme 2).

All derivatives of series A (**6a−6f**) contain a primary, secondary, or cyclic alkyl side chain at the *N*-heterocyclic unit with varying substituents and side chain length. To additionally investigate the influence of the substituents at the biphenyl ring system, different fluorine and alkyl fluorine substituted systems were synthesized with respect to the intended ^{18}F-fluorination.

In general, the synthesis of the compounds **6a−6f** of series A (Scheme 1) started with differently substituted 2-bromophenyl substrates (**1a−1b**), which were converted to the corresponding boronic acids (**2a−2b**; **2c** was commercially available) using *n*-BuLi and trimethyl borate. Following Suzuki cross coupling with commercially available methyl 4-bromo-3-methylbenzoate afforded the corresponding biaryl units (**3a−3c**). To couple the biaryl units with the benzopyrrolodiazepine moiety, the methyl ester functionality was hydrolyzed and converted to its acid chloride. Subsequent reaction with 10,11-dihydro-5*H*-pyrrolo-[2,1-*c*][1,4]benzodiazepine, **8**, synthesized according to reported procedures,[28−30] provided the desired biaryl functionalized benzopyrrolodiazepines (**4a−4c**). To introduce a carboxyl group solely at the 3-position of the tricycle, aromatic acylation with trichloroacetyl chloride in the presence of Hünig's base was performed followed by a haloform type reaction with aqueous NaOH to give the corresponding carboxylic acids (**5a−5c**). The final amidation could be effectively achieved by treating **5a−5c** with 1-ethyl-3-(3-dimethylamino-propyl) carbodiimide hydrochloride (EDCI) and 1-hydroxybenzotriazole (HOBt) as coupling agents followed by the addition of the corresponding amine. For some substrates, the use of (1-cyano-2-ethoxy-2-oxoethylidenaminooxy)dimethylamino-morpholino-carbenium hexafluorophosphate (COMU) or (benzotriazol-1-yl)-*N*,*N*,*N*′,*N*′-tetramethyluronium tetrafluoroborate (TBTU) proved to be superior to the combination of EDCI/HOBt.

For some of the derivatives, the synthetic route was slightly changed. Thus, the synthesis of **6c** was accomplished by fluorination of **6** using one equivalent of diethylaminosulfur trifluoride (DAST). Compound **6e** was synthesized by *N*-methylation of **6d**. Derivative **7** with the 4-tosyloxyethyl side chain was synthesized as a precursor compound for the intended radiosynthesis of [^{18}F]**6b**. The synthetic route started from the benzyl protected 2-(2-bromophenyl)-ethanol **1g**, which was converted to the corresponding boronic acid **2g** for subsequent Suzuki coupling. After haloform type reaction and amidation with diethanolamine, the two primary hydroxyl groups of the resulting derivative **6g** were protected as methyloxymethyl ether to avoid side reactions during radiosynthesis. To introduce an appropriate leaving group for nucleophilic radiofluorination, the benzyl protecting group of the ethoxy side chain was removed by hydrogenolysis and replaced by a tosylate function (**7**).

The synthetic route for the series B derivatives **12a−12d**, **13a**, **13b**, and **14** is shown in Scheme 2. The biaryl carboxylic acid **9**, obtained after fluorination of 2-(2-bromo-phenyl)-ethanol followed by Suzuki coupling with the corresponding boronic acids **2b** and subsequent methyl ester hydrolyses, served as starting material. For the synthesis of **12a−12d**, the reaction sequence of carboxylation and amide formation was applied. The required 1,2,3,4-tetrahydro-pyrrolo[1,2-*a*]pyrazine

DOI: 10.1021/acs.jmedchem.5b01080
J. Med. Chem. XXXX, XXX, XXX−XXX

was synthesized as reported[31] via in situ formation of formaldehyde imine of 2-(1*H*-pyrrol-1-yl)ethanamine, followed by an intramolecular aza-Friedel–Crafts reaction. The synthesis of **12a** and **12b** was accomplished by amidation of the carboxylic acid with the appropriate secondary amine. To gain access to **12d**, the 4-amino-1-Boc-piperidine was used for amidation followed by Boc deprotection. In the same way, mono-Boc-protected piperazine was introduced to obtain **12c**. Boc-protected piperazine was also utilized for the synthesis of **14**. After amidation and deprotection, the secondary amine **11** was finally alkylated with 2-bromoethanol to obtain the product **14**. Compound **13a** was synthesized by amide formation with 4-piperidone followed by reductive amination using diethanolamine. A side product of this reaction obtained by reduction of the ketone functionality to the corresponding secondary alcohol was derivative **13b**.

2.2. Binding Affinity and Estimation of BBB Permeability in Vitro. For determination of the binding affinities of the new derivatives toward hOTR, competitive binding studies were performed using a cell line stably transfected with hOTR gene and [^{3}H]oxytocin as radioligand. The calculated K_i values are summarized in Table 1.

Table 1. In Vitro Binding Affinity, Lipophilicity, and Permeability Data of New Derivatives

compd	K_i [nM][a]	lipophilicity (log D)[b]	permeability (P_m)[c]
		Series A	
6	8.7 ± 1.1	3.21 ± 0.02	3.21 ± 1.23
6a	21.5 ± 8.8	3.31 ± 0.04	4.49 ± 0.80
6b	13.3 ± 7.1	3.14 ± 0.01	6.28 ± 5.64
6c	17.7 ± 5.1	4.89 ± 0.30	24.70 ± 8.81
6d	96.6 ± 7.5	4.18 ± 0.18	34.20 ± 9.32
6e	27.3 ± 6.4	5.20 ± 0.36	25.71 ± 3.49
6f	66.3 ± 14.9	4.08 ± 0.16	7.09 ± 3.06
		Series B	
12a	>1000	nd[d]	nd
12b	>1000	nd	nd
12c	>1000	nd	nd
12d	>1000	nd	nd
13a	>1000	nd	nd
13b	>1000	nd	nd
14	>1000	nd	nd

[a] K_i values in nM (mean ± SD, $n \geq 2$) were derived from IC_{50} values according to the Cheng–Prusoff equation;[32] K_D ([^{3}H]oxytocin) = 2.56 ± 0.95 nM. [b] Log D values (mean ± SD, $n \geq 3$, pH 7.4) were determined by HPLC.[33] [c] P_m values (mean ± S.D., $n \geq 3$) were determined by IAM-chromatography.[34] [d] nd: not determined.

Compounds **6a**, **6b**, and **6c** bind with only slightly lower affinity to hOTR compared to the lead structure **6**. This indicates that minor structural modifications at the biphenyl moiety and at the carbamide functionality are well accepted by the receptor binding site. In contrast, a more pronounced modification of the substituents at the nitrogen of the carbamide function results in a remarkable decrease in binding affinities (**6d** and **6f**). Considering the compounds of series B, we observed almost no relevant interaction with the hOTR (K_i values of >1 μM), which is probably caused by the exchange of the benzopyrrolodiazepine moiety.

To estimate the BBB permeability of the new derivatives, their lipophilicity and permeability was investigated using two different HPLC methods. An established criterion for a passive diffusion of molecules through the BBB is the lipophilicity with a log P or log D value in the range of 1 to 4.[35−37] The log D values of the derivatives of series A (Table 1) were determined according to the HPLC method of Donovan and Pescatore.[33] The log D values of **6**, **6a**, and **6b** are in the range of 3.1−3.3, which indicates at least a moderate passage across the BBB.[35,36] Compounds **6c**−**6f** are considerably more lipophilic with values of >4.1. On one hand, a higher lipophilicity is assumed to enhance the passive diffusion across biological membranes but also increases plasma protein binding which might decrease drug availability. In addition, P. Wils and co-workers[38] have shown that the transport of a drug across intestinal epithelial cells is decreased with increasing lipophilicity (log D values ranging from 3.5 to 5.2), a phenomenon which was explained by successive aqueous−lipid interphases that a higher lipophilic drug has to cross. Correspondingly, a parabolic relationship exists between lipophilicity and brain uptake,[39,40] making derivatives with higher log D values unsuitable as ligands for PET imaging in brain.

Lipophilicity is only one of several physicochemical parameters when discussing BBB permeability, and recent studies have shown that log D values are not generally appropriate predictors for BBB penetration.[41] Therefore, we performed in addition permeability (P_m) measurements according to Taillardat-Bertschinger et al. using immobilized artificial membrane (IAM) chromatography.[34,42] Those IAMs mimic the lipid environment of cell membranes and are formed by synthetic phospholipid analogues covalently bound on the silica support. This modified stationary phase is packed as a solid matrix in a liquid chromatography column. The calculated P_m value correlates with the retention time of the tested compound in the chromatogram. For the IAM measurements of the derivatives of series A, an IAM.PC.DD2 column was used in isocratic mode with phosphate buffer and acetonitrile in different ratios. Data analysis was performed as described in detail in the Experimental Section. As basis, a series of 20 reference compounds was investigated which comprise molecules known to penetrate the BBB by passive diffusion[43] (e.g., raclopride 0.1 ± 0.01, DASB 0.4 ± 0.15, fluoroethylcarfentanil 1.5 ± 0.58, altanserin 2.2 ± 0.8, and elacridar 4.0 ± 2.7). Accordingly, P_m values between 0 and 4 obtained with this test system allowed expectation of a good BBB penetration.[43]

Table 1 shows the P_m values of the derivatives of series A. Within this series, **6** is expected to be the compound with the highest BBB permeability (P_m value of 3.21). As mentioned earlier, this compound was described to be brain penetrable[27] and was therefore chosen as lead structure for the current study. By contrast, the P_m values of compounds **6c**, **6d**, and **6e** are considerably higher (P_m = 24 to 34) and indicate poor permeability. This could be caused by the high lipophilicity of these derivatives hampering the transport of the compounds across a membrane as mentioned.[38] For the derivatives **6a**, **6b**, and **6f**, a moderate BBB permeability may be expected according to P_m values between 4.5 and 7.

On the basis of the highest in vitro binding affinity in combination with the moderate lipophilicity and permeability data, **6b** was selected as candidate for further ^{18}F-labeling and in vivo investigation.

2.3. Radiochemistry. The new radioligand [^{18}F]**6b** was prepared in a two-step synthesis by nucleophilic substitution of a methoxymethyl (MOM) ether protected tosylate precursor (**7**) using anhydrous K[^{18}F]F-$K_{2.2.2}$-carbonate complex in

DOI: 10.1021/acs.jmedchem.5b01080
J. Med. Chem. XXXX, XXX, XXX−XXX

Scheme 3. ^{18}F-Radiolabeling of [^{18}F]**6b**[a]

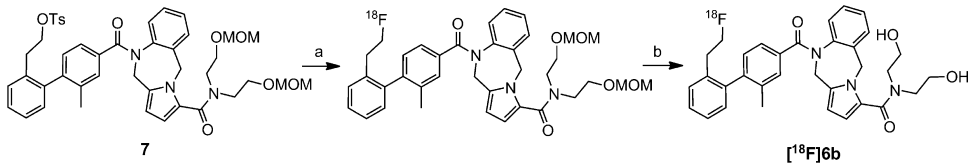

[a]Reagents and conditions: (a) [^{18}F]F^-/$K_{2.2.2}$/K_2CO_3, ACN, with thermal heating (90 °C) or microwave heating (85−95 °C; 75 W); (b) 1 mL 2.0 M HCl, with thermal heating (90 °C) or microwave heating (75−85 °C, 50 W).

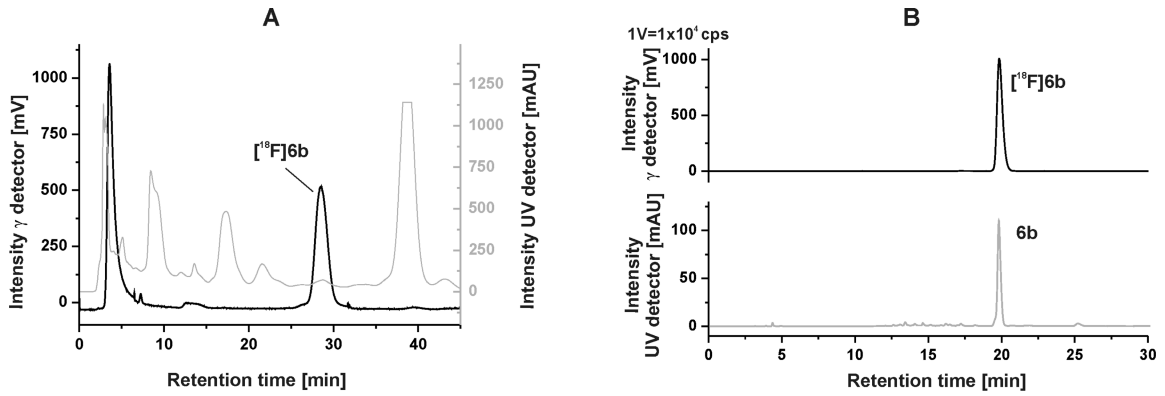

Figure 2. (A) Semipreparative UV- and radio-HPLC chromatograms of [^{18}F]**6b** (conditions: Reprosil-Pur C18-AQ, 250 mm × 10 mm, 44% ACN/20 mM NH_4OAc_{aq}, 4 mL/min). (B) Analytical UV- and radio-HPLC chromatograms of the final product of [^{18}F]**6b** spiked with the reference **6b** (conditions: Reprosil-Pur C18-AQ, 250 mm × 4.6 mm, gradient with eluent A 10% ACN/20 mM NH_4OAc aq and eluent B 90% ACN/20 mM NH_4OAc aq: 0−5′ 100% A, 5−10′ up to 55% B, 10−25′ 55% B, 25−30 up to 100% B, 30−40′ 100% B, 40−45′ up to 100% A, and 45−55′ 100% A).

acetonitrile followed by the deprotection of the two hydroxyl groups using aqueous HCl (Scheme 3).

The ^{18}F-labeling process was investigated under thermal and microwave heating. In general, higher labeling yields in shorter reaction times were achieved under microwave conditions. Using 75 W and a temperature interval of 85−95 °C, the formation of the product was completed within 6−9 min and labeling yields of 67.8 ± 9.4% (n = 11) were achieved. By contrast, under conventional heating at 90 °C, 15 min reaction time was needed until no further increase of labeled product was observed, resulting in labeling yields of 51.7 ± 14.0% (n = 10). Beside [^{18}F]fluoride, no radioactive byproduct was observed under both conditions tested. Moreover, the precursor remained quite stable as proven by HPLC. The deprotection step was also investigated with the two heating methods and different concentrations of hydrochloric acid (0.5, 1.0, and 2.0 M HCl each 1 mL). Using 1 mL of 2.0 M HCl and microwave settings of 50 W/75−85 °C, the deprotection was completed within 5 min. When lower concentrations of HCl were used, longer reaction times were needed. Also for thermal heating at 90 °C, 2.0 M HCl was most appropriate, however, 15 min reaction time was necessary to remove both protecting groups quantitatively. With increasing reaction time the formation of a byproduct (<5%) was observed, which appeared to be slightly more lipophilic than the product according to HPLC analysis.

For isolation of [^{18}F]**6b**, the reaction mixture was neutralized with appropriate amounts of 6.0 M NaOH and injected into the semipreparative HPLC system. The product was collected at a retention time of 27−30 min (A in Figure 2), purified using solid phase extraction on an RP cartridge, and formulated in sterile isotonic saline containing 10% of EtOH for better solubility. Analytical HPLC of the final product, spiked with the unlabeled reference compound, confirmed the identity of [^{18}F]**6b** (B in Figure 2). Finally, the radiotracer was obtained with a radiochemical purity of ≥97% in radiochemical yields of 20.9 ± 4.1% (n = 4, decay corrected) with thermal heating and 26.9 ± 4.7% (n = 6, decay corrected) with microwave heating and specific activities between 35−160 GBq/μmol. Because of the short reaction time and the slightly higher radiochemical yield, the microwave heating system was preferred for the radiosynthesis of [^{18}F]**6b**.

The in vitro stability of the radiotracer was investigated by incubation at 40 °C in the following solutions: (i) 0.9% aq NaCl, (ii) phosphate-buffered saline (PBS), and (iii) pig plasma samples. [^{18}F]**6b** proved to be stable in all media, and no defluorination or degradation was observed within 30 min of incubation time.

The n-octanol-buffer partition coefficient (log D at pH 7.4) of [^{18}F]**6b** was determined for the n-octanol/PBS system by the shake-flask method. The obtained value of 2.87 ± 0.15 (n = 3) is slightly lower than the log D value of 3.14 determined by the HPLC method for the nonradioactive reference compound **6b**.

2.4. In Vitro Affinity and Plasma Free Fraction of [^{18}F]6b. The equilibrium dissociation constant of [^{18}F]**6b** was determined in a homologous competitive binding experiment with K_D = 12.3 nM, which is consistent with the above-reported K_i value of 13.3 nM for the nonradioactive reference compound **6b**.

The plasma free fraction f_p of [^{18}F]**6b**, determined by ultrafiltration of a plasma sample prepared from pooled pig blood and incubated with the radiotracer, was 0.02. This value corresponds with the log D value and indicates sufficient availability of the radiotracer for penetration of the BBB.

2.5. In Vitro Autoradiographic Studies. The distribution of binding sites of [^{3}H]oxytocin and [^{18}F]**6b** in porcine brain is shown in parts A and B of Figure 3, respectively. For [^{18}F]**6b**, we detected the following ranking order: chiasma opticus (CO)

DOI: 10.1021/acs.jmedchem.5b01080
J. Med. Chem. XXXX, XXX, XXX−XXX

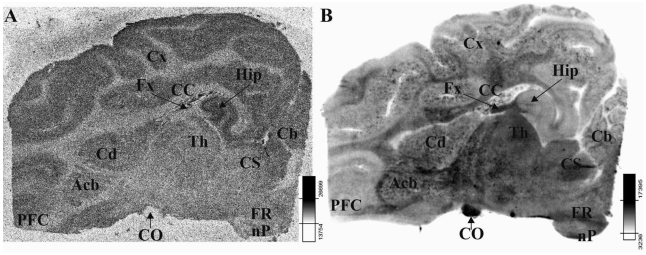

Figure 3. Distribution of the binding sites of (A) [^{3}H]oxytocin (6 nM) and (B) [^{18}F]**6b** (~10 nM) in porcine brain in vitro. Abbreviations: Acb = nucleus accumbens, Cb = cerebellum, CC = corpus callosum, Cd = nucleus caudatus, CO = chiasma opticus, Cx = cortex, CS = colliculus superior, Fx = fornix, FR = formatio reticularis, Hip = hippocampus, nP = nuclei pontis, Th = thalamus, PFC = prefrontal cortex.

> fornix (Fx) > basal ganglia (Acb, Cd) ~ brainstem (FR, nP) > corpus callosum (CC) > cerebellum (Cb) ~ hippocampus (Hip) ~ cortex (Cx) > prefrontal cortex (PFC). By contrast, for [^{3}H]oxytocin, a clearly different pattern was detected: Hip > Cx > Cb ~ PFC > Cd > Th ~ Acb > Fx ~ CC > CO. This quite sparse and very restricted distribution has also been observed in the human and the brain of the titi monkey by [^{125}I]OVTA and [^{3}H]oxytocin autoradiography.[4,44] Therefore, we supposed that these results suggest binding of [^{18}F]**6b** to both OTR as well as other targets. To test this assumption, we performed appropriate competitive binding studies. We noticed a considerable and overall reduction of binding sites of [^{18}F]**6b** by the $GABA_A$ receptor ligand THIP and a localized reduction by oxytocin and the glutamate receptor ligand L-quisqualic acid. In selected brain regions, the binding of [^{18}F]**6b** was both increased and decreased by the vasopressin receptor ligands tolvaptan and SR49059 as well as the σ1/2 receptor ligand siramesine (data not shown). We hypothesize that this substantial off-target binding can be related to the presence of the 1,4-benzodiazepine moiety in [^{18}F]**6b**. In particular, 1,4-benzodiazepine derivatives have been used among others as anxiolytic, hypnotic, anticonvulsant, or antiarrhythmic drugs as well as inhibitors or ligands of a variety of GPCRs such as cholecystokinin, fibrinogen, integrin, vasopressin, bradykinin, or κ-opioid receptors.[45] It might be expected that such features hamper the applicability of benzodiazepine-related OTR ligands such as [^{18}F]**6b** for the PET imaging of OTR in the central nervous system.

2.6. Metabolism of [^{18}F]6b. The metabolism of [^{18}F]**6b** was investigated in plasma samples of female CD1 mice obtained at 30 min pi of the radiotracer. Figure 4 shows a typical analytical HPLC chromatogram of the metabolite profile of the radiotracer. For preparation of RP-HPLC samples, the proteins were precipitated and extracted two times with ACN, with a reproducible recovery of ~82% of the starting radioactivity in the supernatant. We assume that the radioactivity remaining in the pellet mainly attributes to hydrophilic radiometabolites. To verify this assumption, a plasma sample was incubated in vitro with the parent radiotracer and processed under identical conditions as the in vivo experiments. As a result, in vitro more than 99% of the radiotracer could be transferred into the supernatant, leading to the conclusion that the radiotracer is recovered quantitatively also in the in vivo samples. On the basis of this finding, we were able to correct the percentage of intact radiotracer in dependence of the recovery. Therefore, the intensities (mV/min; correlating to the count rates) of each signal in the radio-HPLC chromatograms were summed and related to 82%. This ratio was used to calculate the percentage of intact radiotracer based on its peak intensity in the chromatogram. Accordingly, 20% of intact radiotracer is available in plasma at 30 min pi, which is slightly less than the uncorrected value of 25%.

During the dynamic PET study in pig, we also determined the fraction of nonmetabolized [^{18}F]**6b** in plasma samples taken at 2, 8, 30, and 60 min pi of the radiotracer and processed them as described for the plasma samples of mouse. The metabolite RP-HPLC profile is comparable to the profile observed for the mouse samples at 30 min pi. However, for samples collected at later time points, we detected a considerable decrease of recovery of radioactivity ranging from 97% at 2 min pi to 64% at 60 min pi. Therefore, the percentage of intact radiotracer at each time point was calculated as described and the corrected values are given in Table 2. Accordingly, intact tracer accounts for 31% of total activity in plasma at 30 min pi.

2.7. In Vivo Characterization of [^{18}F]6b. To assess brain uptake and pharmacokinetics of this type of tricyclic benzodiazepine in more detail, biodistribution of [^{18}F]**6b** was investigated in female CD-1 mice 5 and 30 min after intravenous injection of ~220 kBq of the radioligand. With 0.41% ID/g (SUV = 0.11) at 5 min pi, a rather low brain uptake was observed, followed by a fast washout (0.11% ID/g or SUV = 0.03 at 30 min pi). In addition, we detected high uptake of radioactivity in the pituitary gland (Figure 5; 8.36% ID/g, SUV

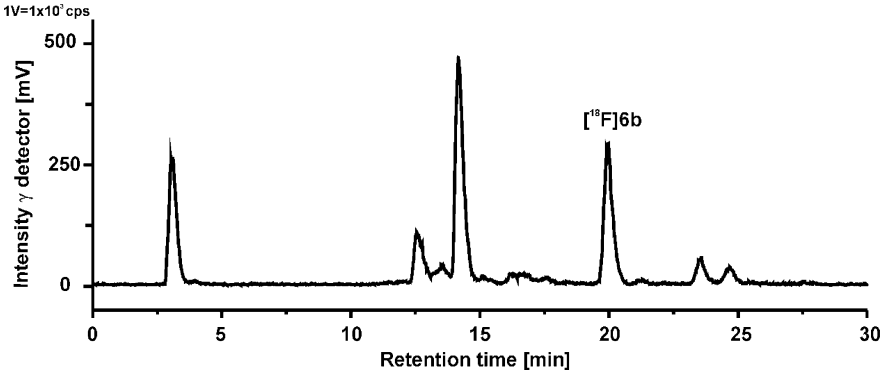

Figure 4. Analytical radio-HPLC chromatogram of a plasma sample of [^{18}F]**6b** 30 min pi. Conditions: Reprosil-Pur C18-AQ; 250 mm × 4.6 mm; flow 1.0 mL/min; gradient mode see Experimental Section.

DOI: 10.1021/acs.jmedchem.5b01080
J. Med. Chem. XXXX, XXX, XXX−XXX

Table 2. Percentage of [^{18}F]6b in Plasma Samples of Pig

time of sampling [min pi]	radioactivity recovery [%]	peak area [^{18}F]6b[a] [mV/min]	peak area total[b] [mV/min]	[^{18}F]**6b** noncorr[c] [%]	[^{18}F]**6b** corr[d] [%]
2	97	461	467	99	96
8	77	55	77	71	55
30	69	76	172	44	31
60	64	11	70	16	10

[a]Values are taken from radio-HPLC chromatograms. [b]Sum of values of all signals taken from each radio-HPLC chromatogram. [c]Percentage values without correlation to the recovery of radioactivity. [d]Percentage values with correlation to the recovery of radioactivity.

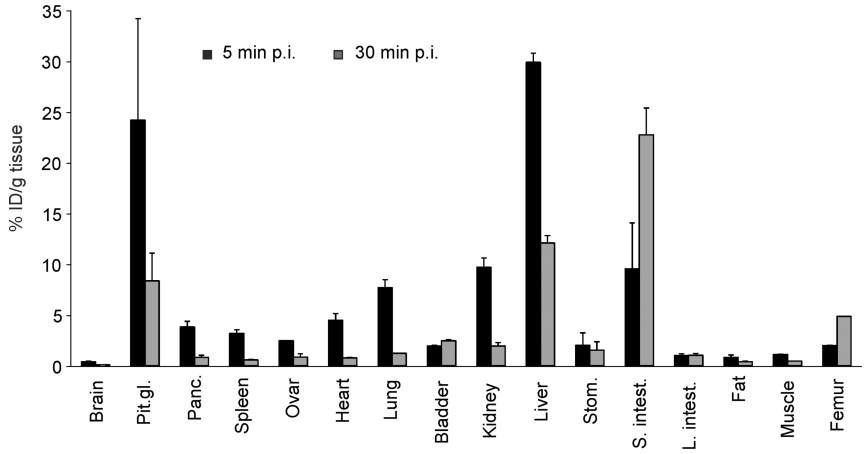

Figure 5. Organ distribution of [^{18}F]**6b** in mice (data are presented as mean values ± sd; n = 2 per time point).

= 2.1 at 30 min pi), a region outside of the BBB with known OTR expression.[46] This uptake might indicate a specific binding of [^{18}F]**6b** to OTRs but could also be caused by the binding to the oxytocin specific carrier protein neurophysin.[8] The excretory organs small intestine and liver showed the highest accumulation of radioactivity at 30 min pi (22.8% ID/g and 12.1% ID/g, respectively). The increasing accumulation in the femur may indicate some defluorination of the radiotracer, although OTR expression has also been found in bone marrow.[47]

To analyze the kinetics of the brain uptake of [^{18}F]**6b** and to assess an interaction of this particular tricyclic benzodiazepine with efflux transporters of the blood–brain barrier, pharmacokinetics was further studied by dynamic PET scans under baseline and blocking conditions in female CD-1 mice. The results obtained by these PET studies revealed a very low uptake of [^{18}F]**6b** in the mouse brain during the 60 min acquisition, with peak radioactivity in whole brain of SUV 0.07 at 5 and 0.04 at 60 min pi (Figure 6). A considerably higher accumulation of radioactivity (SUV 0.7 at 60 min pi) was detected in the pituitary gland. To investigate a possible interaction of [^{18}F]**6b** with the efflux transporter P-glycoprotein (P-gp) as cause for the low brain uptake, additional PET studies under pretreatment with the known P-gp inhibitor cyclosporin[48] were performed. However, neither in brain nor in the pituitary gland of mice was an increase in the uptake of [^{18}F]**6b** observed.

Finally, [^{18}F]**6b** failed to image brain OTR in vivo in mouse, most probably due to lack of brain penetration. However, the log D and P_m values at physiological pH are assumed to be compatible with at least a moderate brain permeation of [^{18}F]**6b**. In addition, the absence of an effect of cyclosporine on the brain uptake of the radiotracer indicates no substantial interaction of [^{18}F]**6b** with the P-gp. However, an important aspect of preclinical evaluation of brain targeting PET

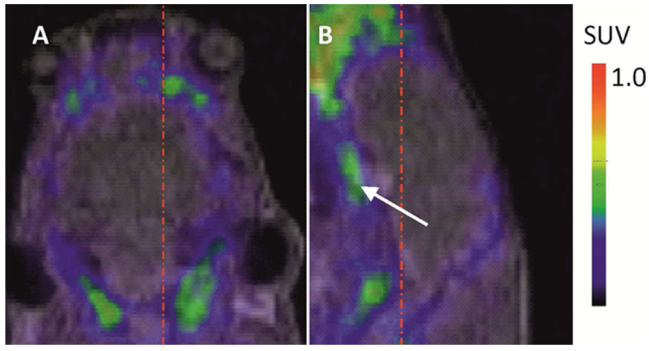

Figure 6. Representative image of a PET scan of [^{18}F]**6b** at 60 min pi of a brain of a female CD-1 mouse. The arrow is pointing to the pituitary gland and the crosshairs designating the slice location of the transverse and sagittal slice. (A) Transverse slice. (B) Sagittal slice.

radiotracers is species specificity as reflected by, e.g., higher brain uptake of [^{11}C]GR205171 and [^{18}F]altanserin in humans and monkey than in rats[49] and of the α7 nicotinic acetylcholine receptor ligand [^{18}F]NS14490 in pig than in mouse.[50,51] To test if such behavior is also relevant for the tricyclic benzodiazepines under investigation in the current study, we decided to proceed with the evaluation of [^{18}F]**6b** in one pig.

Although this single PET study in pig confirmed a low BBB permeability of [^{18}F]**6b** with a maximum SUV of 0.34 in brain at 30 min pi, this value reflects an about 10-fold higher brain uptake in pig than in mouse (SUV 0.03–0.04 at 30 min pi). Interestingly, the uptake in the olfactory bulb (SUV = 0.33 at 30 min pi) was considerably higher than in other brain regions, which is consistent with a comparably high OTR expression found in rats.[7]

Despite a slightly better penetration of [^{18}F]**6b** across the BBB in pig than in mouse, the total brain uptake is rather low and hampers reliable imaging and quantification of OTR in the

DOI: 10.1021/acs.jmedchem.5b01080
J. Med. Chem. XXXX, XXX, XXX–XXX

living brain. To disclose the reason for the low brain penetration is ambitious. As often reported, the magnitude of brain uptake of a compound is mainly determined by its size, lipophilicity, H-bonding capacity, polar surface area (PSA), and molecular flexibility.[36,37] The lipophilicity of [^{18}F]**6b** with an experimentally determined log *D* value of 2.8 is in the range for BBB penetrating compounds[35,36] and gives therefore no valuable information. However, with a molecular weight of 555 g/mol, the size of the compound is considerably higher than the limit of 400 g/mol, reported by Waterbeemd et al. for a set of 125 CNS-active and inactive drugs.[37] In this study, additional to the size dependency, also the PSA was specified as significant criterion for BBB penetration and estimated to be <90 Å^2 for CNS-active drugs. Later on, Kelder et al. suggested an even more stringent cutoff of PSA < 60 Å^2 based on calculations with a data set of more than 700 CNS-active drugs.[52] Therefore, with a calculated TPSA (topological PSA) value[53] of 86 Å^2 for [^{18}F]**6b**, a passage across the BBB seems to be not favored (TPSA values are comparable to PSA values[54]). Because the PSA is defined as the surface area occupied by nitrogen and oxygen atoms and the polar hydrogens attached to them,[55] it also reflects the hydrogen bonding capacity and polarity of a compound. Thus, in particular, the two OH groups, acting as H-bond donors, contribute to the high TPSA value. Additionally, the free rotation and steric availability of these aliphatic OH groups may hamper the diffusion across a lipophilic membrane. We are aware that the requirements for BBB penetration are more complex and not only simply related to physicochemical properties. However, these considerations may serve as a first explanation for the observed poor brain uptake of [^{18}F]**6b**.

3. SUMMARY AND CONCLUSION

With the 10,11-dihydro-5*H*-benzo[*e*]pyrrolo[1,2-*a*][1,4]-diazepine derivative **6b**, a novel ligand with high affinity for the oxytocin receptor was synthesized and radiolabeled with fluorine-18 and the binding affinity in vitro and pharmacokinetics in vivo were evaluated.

Because of the very low brain uptake of [^{18}F]**6b** in mouse and pig, this radiotracer is not suitable for examining the oxytocin receptor in the living brain. The molecular size of [^{18}F]**6b** and the relatively high polar surface area with two easily accessible OH groups might account for the low brain penetration. This is also reflected by the in vitro permeability (P_m) determined by IAM chromatography, which is not in the ideal range of brain penetrating compounds.[43] The lipophilicity, characterized by the log *D* value, was not a good predictor for BBB penetration of [^{18}F]**6b**. Moreover, on the basis of blockade PET studies in mice, we could show that [^{18}F]**6b** does not significantly interact with the efflux transporter P-gp, a further parameter that can strongly influence the brain uptake of a compound.

Furthermore, in vitro autoradiographic blocking studies on porcine brain indicated interaction of the radioligand at binding sites of several off-target receptors, which hampers the applicability of [^{18}F]**6b** as specific OTR-PET tracer. This low selectivity is assumed to be caused by the 1,4-benzodiazepine moiety in [^{18}F]**6b**, which is part of numerous drugs and ligands for several GPCRs. However, as we have shown with the series B compounds, this 1,4-benzodiazepine moiety is essential for high affinity to the OTR binding site.

Finally, we conclude that the selected OTR antagonist **6** is not suitable as lead structure for the development of PET tracers for the oxytocin receptor because of the observed poor brain penetration and limited target selectivity of its analogue [^{18}F]**6b**.

4. EXPERIMENTAL SECTION

4.1. Organic Chemistry. *General.* All reactions were carried out under argon atmosphere, in dry glassware, with dried solvents and anhydrous conditions, unless otherwise stated. Reagents were purchased with a minimum commercial quality of 95% and used without further purification. Analytical thin layer chromatography (TLC) was performed on 0.25 mm silica gel plates Alugram SIL G/UV$_{254}$ (Machery-Nagel, Germany). The spots were visualized by using UV light or staining with ninhydrin, phosphomolybdic acid, or vanillin followed by heating. Column chromatography for purification of the crude products was carried out on silica gel (60, particle size 0.040−0.063 mm, Machery-Nagel). NMR spectra were recorded on Bruker AV 500 Ultra instruments and calibrated using residual nondeuterated solvents as an internal reference. Following abbreviations were used to describe the multiplicities: s = singlet, d = doublet, t = triplet, q = quartet, m = multiplet, dt = doublet of triplet, td = triplet of doublet, dd = doublet of doublet.

Analysis of all final compounds was performed by TLC, MS, and ^{1}H- and ^{13}C NMR spectroscopy. The purity of the final compounds was ≥95% and was confirmed by LC/MS analysis employing a Thermo SCIENTIFIC Ultimate 3000 system consisting of a quaternary pump, a diode array detector, and an autosampler. Electrospray ionization mass spectra were obtained using a MSQ mass detector (Thermo SCIENTIFIC). An Ascentic Express Peptide ES-C18 column 150 mm × 2.1 mm (SUPELCO) was used in gradient mode (eluent: acetonitrile/H$_2$O + 0.1% HCOOH (v); 5% to 100% ACN over 12 min with a flow rate of 0.4 mL/min), and the chromatograms were monitored at 220 nm.

Chemical names of compounds were generated by ChemDraw Ultra 10.0.

TPSA values were calculated using the free Molecular Property Calculation service of Molinspiration (molinspiration.com).

*Synthesis of the Precursor **7**. Benzyl 2-(2-Bromophenyl)ethyl Ether (**1g**).* A solution of 7.44 g (37 mmol) of 2-bromophenylethyl alcohol in 60 mL of THF was added under argon atmosphere to an ice-cooled suspension of 2.25 g (56 mmol, 60% in mineral oil) NaH in 60 mL of THF. After stirring for 30 min at rt, the suspension was heated to 50 °C for 30 min and cooled to 0 °C for the addition of 5.4 mL (7.77 g, 45 mmol) benzyl bromide. The reaction mixture was stirred at rt overnight. Then 50 mL of H$_2$O were slowly added and the organic solvent was removed under reduced pressure. The aqueous layer was extracted with diethyl ether, and the organic layer was dried over Na$_2$SO$_4$. Column chromatography (petroleum ether (PE): diethyl ether = 15:1) of the crude product afforded 10 g (93%) of **1g** as a colorless oil. ^{1}H NMR (500 MHz, CDCl$_3$) δ [ppm]: 3.09 (t, J = 7.0 Hz, 2H), 3.73 (t, 7.0 Hz, 2H), 4.55 (s, 2H), 7.08 (td, J = 7.5 Hz, J = 1.5 Hz, 1H), 7.24 (td, J = 7.5 Hz, J = 1.5 Hz, 1H), 7.27−7.36 (m, 6H), 7.54 (dd, J = 8.0 Hz, J = 1.0 Hz, 1H).

*Benzyl 2-(2-Boronophenyl)ethyl Ether (**2g**).* To a solution of 8.9 g (31 mmol) of **1g** in 150 mL of dry THF, *n*-BuLi (14.8 mL, 2.5 M in *n*-hexane) was added at −78 °C and the mixture was stirred for 1 h at this temperature. After addition of 4.1 mL (3.8 g, 37 mmol) of trimethyl borate, the cooling bath was removed and the reaction mixture was stirred at rt overnight, quenched with 100 mL of 1.0 M aqueous HCl, and stirred for 1 h. The organic layer was separated, and the aqueous layer was extracted with CH$_2$Cl$_2$ (2 × 100 mL). The combined organic layers were washed with brine and dried over Na$_2$SO$_4$ and the solvent was removed in vacuum. The obtained 7.9 g (99%) of the crude product **2g** was used in the next step without any further purification.

*2′-(2-Benzyloxyethyl)-2-methylbiphenyl-4-carboxylic Acid Methyl Ester (**3g**).* A stirred solution of 7.9 g (31 mmol) of **2g**, 7.0 g (31 mmol) of methyl 4-bromo-3-methylbenzoate, and 14.2 g (134 mmol) of Na$_2$CO$_3$ in 360 mL of H$_2$O/ethyl alcohol/toluene (1:1:2) was degassed for 30 min with argon. The catalyst Pd(PPh$_3$)$_4$ (1.78 g, 1.5

DOI: 10.1021/acs.jmedchem.5b01080
J. Med. Chem. XXXX, XXX, XXX−XXX

mmol) was added, and the obtained yellow solution was refluxed at 90 °C for 14 h. After cooling to rt, 150 mL of ethyl acetate (EtOAc) was added and the aqueous layer was separated. The organic layer was washed with brine and dried over Na_2SO_4. After removal of the solvents, the crude product was purified by column chromatography (*n*-hexane:EtOAc = 10:1) to yield 9.5 g (85%) of **3g** as colorless oil. ^{1}H NMR (500 MHz, $CDCl_3$) δ [ppm]: 2.06 (s, 3H), 2.60 (dt, J = 14.0 Hz, J = 7.0 Hz, 1H), 2.75 (dt, J = 14.0 Hz, J = 7.0 Hz, 1H), 3.45 (t, J = 7.5 Hz, 2H), 3.95 (s, 3H), 4.37 (s, 2H), 7.06 (dd, J = 7.5 Hz, J = 1.5 Hz, 1H), 7.14 (d, J = 7.5 Hz, 1H), 7.16−7.18 (m, 2H), 7.24−7.36 (m, 6H), 7.85 (dd, J = 8.0 Hz, J = 1.5 Hz, 1H), 7.93 (s, 1H).

*10,11-Dihydro-5H-pyrrolo[2,1-c][1,4]benzodiazepine (**8**).* Compound **8** was synthesized according to the literature[28−30] by *N*-alkylation of pyrrole-2-carboxaldehyde with 2-nitrobenzyl bromide followed by reductive ring closure of 1-(2-nitrobenzyl)-2-pyrrolecarboxaldehyde. ^{1}H NMR (500 MHz, $CDCl_3$) δ [ppm]: 4.18 (br s, 1H), 4.46 (d, J = 4.0 Hz, 2H), 5.19 (s, 2H), 6.02−6.05 (m, 2H), 6.49 (dd, J = 8.0 Hz, J = 1.0 Hz, 1H), 6.63 (td, J = 7.5 Hz, 1.0 Hz, 1H), 6.68−6.69 (m, 1H), 6.98−7.05 (m, 2H).

*(5H,11H-Benzo[e]pyrrolo[1,2-a][1,4]diazepin-10-yl)-[2′-(2-benzyloxyethyl)-2-methylbiphenyl-4-yl]methanone (**4g**).* To a stirred solution of 9.5 g (26 mmol) of **3g** in 190 mL of THF, a solution of 96 mL of 1.0 M aqueous NaOH was added and the mixture was stirred under reflux overnight. The complete consumption of the starting material was confirmed by TLC (PE:*n*-hexane = 9:1). After removal of THF, 1.0 M aqueous HCl was added to adjust a pH value of 3 and the product was extracted with EtOAc. The combined organic layers were dried over Na_2SO_4. Removal of the solvent afforded 8.5 g (94%) of the corresponding carboxylic acid as white solid, which was used directly in the next step; mp 61−64 °C. ^{1}H NMR (500 MHz, DMSO-d_6) δ [ppm]: 2.00 (s, 3H), 2.50 (dt, J = 14.0 Hz, J = 7.0 Hz, 1H), 2.67 (dt, J = 14.0 Hz, J = 7.0 Hz, 1H), 3.40 (t, J = 7.0 Hz, 2H), 4.31 (s, 2H), 7.06 (dd, J = 7.5 Hz, J = 1.5 Hz, 1H), 7.12−7.18 (m, 3H), 7.22−7.30 (m, 4H), 7.33 (td, J = 7.5 Hz, J = 1.5 Hz, 1H), 7.40 (m, 1H), 7.78 (dd, J = 8.0 Hz, J = 1.5 Hz, 1H), 7.87 (d, J = 1.5 Hz, 1H), 12.93 (br s, 1H).

A solution of 4.5 g (13 mmol) of 2′-(2-benzyloxy-ethyl)-2-methylbiphenyl-4-carboxylic acid in 25 mL of thionyl chloride was refluxed under argon atmosphere for 2 h. The excess of thionyl chloride was removed under vacuum, and the residue was diluted three times with 10 mL of toluene followed by removal of the solvent. The resultant acid chloride was dissolved in 25 mL of CH_2Cl_2 and added dropwise to an ice-cold solution of 2.8 g (15 mmol) of **8** and 5.1 mL (30 mmol) of Hünig's base in 100 mL of CH_2Cl_2. The cooling bath was removed, and the mixture was stirred at rt overnight. After hydrolysis with 50 mL of H_2O, the aqueous layer was extracted three times with CH_2Cl_2. The combined organic layers were dried over Na_2SO_4, filtered, and concentrated in vacuum. The crude product was purified by column chromatography (PE:EtOAc = 4:1 to 1:1) to obtain 5.6 g (84%) of **4g** as colorless oil. ^{1}H NMR (500 MHz, DMSO-d_6) δ [ppm]: 1.83 (s, 3H), 2.38 (dt, J = 14.0 Hz, J = 7.0 Hz, 1H), 2.57 (dt, J = 14.0 Hz, J = 7.0 Hz, 1H), 3.30 (t, J = 7.0 Hz, 2H), 4.27 (s, 2H), 5.21 (br s, 2H), 5.31 (br s, 2H), 5.93 (dd, J = 3.0 Hz, J = 3.0 Hz, 1H), 5.97 (br s, 1H), 6.83−6.86 (m, 2H), 6.90−6.97 (m, 2H), 7.00−7.07 (m, 2H), 7.10−7.17 (m, 3H), 7.21−7.36 (m, 7H), 7.45 (d, J = 7.5 Hz, 1H).

*1-[10-[2′-(2-Benzyloxyethyl)-2-methylbiphenyl-4-carbonyl]-10,11-dihydro-5H-benzo[e]pyrrolo[1,2-a][1,4]diazepin-3-yl]-2,2,2-trichloroethanone (**15**; Intermediate of Reaction Step (e) in Scheme 1).* To an ice-cold solution of 5.5 g (11 mmol) of **4g** in 115 mL of CH_2Cl_2, Hünig's base was added (3.6 mL, 2.7 g, 22 mmol) under argon atmosphere. After the addition of 3.8 mL (6.2 g, 34 mmol) of trichloro acetyl chloride over 10 min, the cooling bath was removed and the mixture was stirred at rt overnight. The reaction mixture was diluted with 50 mL of H_2O, and the aqueous layer was extracted twice with CH_2Cl_2. The combined organic layers were washed with 100 mL of 1.0 M aqueous HCl and 50 mL of brine, dried over Na_2SO_4, filtered, and concentrated to remove the solvent. Column chromatography (PE:EtOAc = 2:1) afforded 6.4 g (92%) of the product **15** as a colorless solid; mp 80−85 °C. ^{1}H NMR (500 MHz, DMSO-d_6) δ [ppm]: 1.84 (s, 3H), 2.38 (dt, J = 14.0 Hz, J = 7.0 Hz, 1H), 2.57 (dt, J = 14.0 Hz, J = 7.0 Hz, 1H), 3.30 (t, J = 7.0 Hz, 2H), 4.28 (s, 2H), 5.30 (br s, 2H), 5.98 (br s, 2H), 6.38 (d, J = 4.5 Hz, 1H), 6.86 (d, J = 8.0 Hz, 1H), 6.90 (d, J = 8.0 Hz, 1H), 6.97 (dd, J = 7.5 Hz, J = 1.5 Hz, 1H), 7.01−7.07 (m, 2H), 7.12 (td, J = 7.5 Hz, J = 1.5 Hz, 1H), 7.15−7.17 (m, 2H), 7.21−7.35 (m, 7H), 7.42 (dd, J = 7.5, J = 1.5 Hz, 1H), 7.47 (d, J = 4.0 Hz, 1H).

*10-[2′-(2-Benzyloxyethyl)-2-methylbiphenyl-4-carbonyl]-10,11-dihydro-5H-benzo[e]pyrrolo[1,2-a][1,4]diazepine-3-carboxylic Acid (**5g**).* To a solution of 6.4 g (10 mmol) of **15** in 200 mL of acetone, 30 mL of 2.5 M aqueous NaOH was added and the mixture was stirred at rt overnight. After removal of the solvent, 25 mL of 2.0 M aqueous HCl was added and the mixture was extracted with EtOAc. The organic layer was dried over Na_2SO_4, filtered, and concentrated to remove the solvent. The crude product was purified by column chromatography (PE:EtOAc = 1:1) to provide 4.5 g (83%) of **5g** as a white solid; mp 64−68 °C. ^{1}H NMR (500 MHz, DMSO-d_6) δ [ppm]: 1.83 (s, 3H), 2.39 (dt, J = 14.0 Hz, J = 7.0 Hz, 1H), 2.58 (dt, J = 14.0 Hz, J = 7.0 Hz, 1H), 3.30 (t, J = 7.0 Hz, 2H), 4.28 (s, 2H), 5.20 (br s, 2H), 5.95 (br s, 2H), 6.12 (d, J = 4.0 Hz, 1H), 6.77 (d, J = 4.0 Hz, 1H), 6.83−6.87 (m, 2H), 6.95−7.02 (m, 3H), 7.09 (t, J = 7.0 Hz, 1H), 7.16 (t, J = 7.0 Hz, 2H), 7.21−7.35 (m, 8H), 12.34 (br s, 1H).

*10-[2′-(2-Benzyloxyethyl)-2-methylbiphenyl-4-carbonyl]-10,11-dihydro-5H-benzo[e]pyrrolo[1,2-a][1,4]diazepine-3-carboxylic Acid Bis(2-hydroxyethyl)amide (**6g**).* A mixture of 2.5 g (4.5 mmol) of **5g**, 0.66 g (6.3 mmol) of diethanolamine, 0.88 g (6.5 mmol) of HOBt, 1.12 g (5.9 mmol) of EDCI, and 1.3 mL (0.99 g, 7.7 mmol) of Hünig's base in 45 mL of DMF was stirred at rt overnight. The mixture was concentrated, diluted with 75 mL of H_2O, and extracted three times with 75 mL of EtOAc. The organic layer was washed twice with 50 mL of a saturated aqueous $NaHCO_3$ solution, dried over Na_2SO_4, filtered, and concentrated to remove the solvent. Purification by column chromatography (CH_2Cl_2:methanol = 95:5) afforded 2.46 g (85%) of **6g** as a white solid. ^{1}H NMR (500 MHz, $CDCl_3$) δ [ppm]: 1.89 (s, 3H), 2.50 (td, J = 7.5 Hz, J = 13.5 Hz, 1H), 2.64 (dt, J = 7.0 Hz, J = 14.0 Hz, 1H), 3.36 (t, J = 7.5 Hz, 2H) 3.44 (br s, 2H), 3.77 (t, J = 5.0 Hz, 4H), 3.88 (br s, 4H), 4.33 (dd, J = 12.0 Hz, J = 14.5 Hz, 2H), 5.30 (br s, 2H), 5.47 (br s, 2H), 6.01 (d, J = 4.0 Hz, 1H), 6.51 (d, J = 4.0, 1H), 6.79−6.85 (m, 2H), 6.96 (d, J = 8.0 Hz, 1H), 7.01 (t, J = 7.0 Hz, 1H), 7.10 (t, J = 7.0 Hz, 1H), 7.17−7.22 (m, 3H), 7.24−7.27 (m, 3H), 7.28−7.31 (m, 3H), 7.45 (dd, J = 1.5 Hz, J = 7.5 Hz, 1H).

*10-[2′-(2-Benzyloxyethyl)-2-methylbiphenyl-4-carbonyl]-10,11-dihydro-5H-benzo[e]pyrrolo[1,2-a][1,4]diazepine-3-carboxylic Acid Bis(2-methoxymethoxyethyl)amide (**16**; Intermediate of Reaction Step (i) in Scheme 1).* A solution of 1.39 g (2.2 mmol) of **6g** in 30 mL of CH_2Cl_2 was cooled on ice, and 1.6 mL (9.5 mmol) of Hünig's base, 65 mg (0.22 mmol) of tetrabutylammonium chloride, and 0.77 mL (9.5 mmol) of bromomethyl methyl ether were added. The resultant solution was allowed to warm to rt and stirred overnight. The mixture was diluted with H_2O, and the separated aqueous layer was extracted with CH_2Cl_2. The combined organic layers were dried over Na_2SO_4, filtered, and concentrated in vacuum. Flash chromatography (PE:EtOAc = 1:1) of the crude product afforded 1.4 g (87%) of **16** as an orange oil. ^{1}H NMR (500 MHz, $CDCl_3$) δ [ppm]: 1.83 (s, 3H), 2.38 (td, J = 7.5 Hz, J = 13.5 Hz, 1H), 2.57 (dt, J = 7.0 Hz, J = 14.0 Hz, 1H), 3.20−3.26 (m, 6H), 3.30 (t, J = 7.0 Hz, 2H), 3.58−3.73 (m, 8H), 4.27 (s, 2H), 4.57 (br s, 3H), 4.63 (br s, 1H), 5.20 (br s, 2H), 5.35 (br s, 2H), 6.05 (d, J = 3.5 Hz, 1H), 6.29 (d, J = 3.5 Hz, 1H), 6.83−6.88 (m, 2H), 6.96 (d, J = 7.0 Hz, 1H), 6.98−7.02 (m, 2H), 7.09 (t, J = 7.0 Hz, 1H), 7.16 (d, J = 7.0 Hz, 2H), 7.21−7.35 (m, 8H).

*10-[2′-(2-Hydroxyethyl)-2-methylbiphenyl-4-carbonyl]-10,11-dihydro-5H-benzo[e]pyrrolo[1,2-a][1,4]diazepine-3-carboxylic Acid Bis(2-methoxymethoxyethyl)amide (**17**; Intermediate of Reaction Step (j) in Scheme 1).* To a degassed solution of 860 mg (1.18 mmol) of compound **16** in 60 mL of methanol, $Pd(OH)_2/C$ (200 mg, 20 wt %, wet, 0.28 mmol) was added. The mixture was vigorously stirred at rt under a hydrogen atmosphere (balloon pressure) for 20 h. TLC analysis (100% EtOAc) indicated the complete consumption of the starting material. The reaction mixture was filtered through Celite and washed with methanol. The filtrate was concentrated and dried in vacuum to give 750 mg (99%) of the titled compound as yellowish viscous oil. The intermediate **17** was used in the next step without any further purification. ^{1}H NMR (500 MHz, DMSO-d_6) δ [ppm]: 1.86 (s,

DOI: 10.1021/acs.jmedchem.5b01080
J. Med. Chem. XXXX, XXX, XXX−XXX

3H), 2.24−2.31 (m, 1H), 2.41−2.47 (m, 1H), 3.24−3.30 (m, 8H), 3.62−3.74 (m, 8H), 4.47 (t, J = 5.0 Hz, 1H), 4.55−4.78 (m, 4H), 5.15 (br s, 2H), 5.35 (br s, 2H), 6.05 (d, J = 3.5 Hz, 1H), 6.29 (d, J = 3.5 Hz, 1H), 6.88 (d, J = 8.0 Hz, 2H), 6.94 (d, J = 7.5 Hz, 1H), 7.02 (d, J = 7.5 Hz, 1H), 7.09 (t, J = 7.5 Hz, 1H), 7.16 (t, J = 7.5 Hz, 1H), 7.21 (td, J = 7.5 Hz, J = 1.5 Hz, 1H), 7.25 (s, 1H), 7.27 (td, J = 7.5 Hz, 1.5 Hz, 1H), 7.31 (dd, J = 7.5 Hz, 1.5 Hz, 1H), 7.36 (d, J = 7.5 Hz, 1H).

*Toluene-4-sulfonic Acid 2-(4′-[3-[Bis(2-methoxymethoxy-ethyl)-carbamoyl]-5H,11H-benzo[e]pyrrolo[1,2-a][1,4]diazepine-10-carbonyl]-2′-methylbiphenyl-2-yl)ethyl Ester (**7**).* A solution of 178 mg (0.93 mmol) of *p*-toluenesulfonyl chloride in 1 mL of CH_2Cl_2 was added under argon atmosphere to an ice-cooled solution of 104 mg (0.16 mmol) of compound **17**, 0.13 mL (0.93 mmol) of triethylamine, and 2 mg (0.02 mmol) of Steglich base (4-DMAP) in 3 mL of CH_2Cl_2. The mixture was stirred at rt overnight. The progress of the reaction was monitored by TLC (*n*-hexane:EtOAc = 1:1). After complete consumption of **17**, the reaction mixture was diluted with H_2O and extracted with CH_2Cl_2. The organic layer was dried over Na_2SO_4, filtered, and concentrated in vacuum. The resulting residue was purified by column chromatography (*n*-hexane:EtOAc = 2:3) to give 101 mg (78%) of **7** as a white solid; mp 75−80 °C. ^{1}H NMR (500 MHz, $CDCl_3$) δ [ppm]: 1.76 (s, 3H), 2.38 (td, J = 7.5 Hz, J = 13.5 Hz, 1H), 2.41 (s, 3H), 2.59 (dt, J = 7.0 Hz, J = 14.0 Hz, 1H), 3.25 (br s, 6H), 3.58−3.73 (m, 8H), 3.78−3.90 (m, 2H), 4.57 (br s, 3H), 4.64 (br s, 1H), 5.20 (br s, 2H), 5.36 (br s, 2H), 6.05 (d, J = 3.5 Hz, 1H), 6.30 (d, J = 3.5 Hz, 1H), 6.67 (d, J = 7.5 Hz, 1H), 6.82 (d, J = 6.0 Hz, 1H), 6.94−6.96 (m, 2H), 7.02 (t, J = 7.0 Hz, 1H), 7.12 (t, J = 7.5 Hz, 1H), 7.22 (s, 1H), 7.23−7.29 (m, 3H), 7.35 (d, J = 7.0 Hz, 1H), 7.41 (d, J = 8.0 Hz, 2H), 7.55 (d, J = 8.0 Hz, 2H). ^{13}C NMR (125 MHz, DMSO-d_6) δ [ppm]: 19.18, 20.95, 31.53, 45.97, 47.03, 54.59, 55.06, 64.65, 65.22, 69.70, 91.44, 92.66, 95.64, 107.61, 110.51, 125.07, 126.67, 126.80, 126.98, 127.28, 127.57, 128.39, 128.41, 128.63, 128.91, 129.12, 129.21, 129.61, 129.97, 132.03, 133.52, 134.67, 134.69, 134.82, 140.13, 141.30, 141.40, 144.73, 163.73, 169.17. LC/MS retention time: 10.80 min. MS (ESI) m/z = 796.2 $[M + H]^+$.

*Synthesis of **6a**. 5′-Fluoro-2-methyl-2′-trifluoromethylbiphenyl-4-carboxylic Acid Methyl Ester (**3a**).* The compound was synthesized using 1.0 g (4.8 mmol) of 5-fluoro-2-(trifluoromethyl)phenylboronic acid according to the procedure for the synthesis of **3g**. The obtained crude product was purified by column chromatography (*n*-hexane:EtOAc = 9:1) to yield 1.4 g (91%) of **3a** as a colorless oil. ^{1}H NMR (500 MHz, $CDCl_3$) δ [ppm]: 2.05 (s, 3H), 3.86 (s, 3H), 7.04 (d, J = 6.5 Hz, 1H), 7.10 (t, J = 6.5 Hz, 1H), 7.30 (s, 1H), 7.42−7.48 (m, 2H), 7.89 (dd, J = 7.5 Hz, J = 5.5 Hz, 1H).

*(5H,11H-Benzo[e]pyrrolo[1,2-a][1,4]diazepin-10-yl)-(5′-fluoro-2-methyl-2′-trifluoromethylbiphenyl-4-yl)methanone (**4a**).* According to the procedure described for the synthesis of **4g**, compound **3a** was hydrolyzed and 0.96 g (3.2 mmol) of the resulting carboxylic acid was used to react with 0.89 g (4.8 mmol) of **8**. The obtained crude product was purified by column chromatography (*n*-hexane:EtOAc = 4:1) to yield 1.4 g (94%) of **4a** as a colorless oil. ^{1}H NMR (500 MHz, DMSO-d_6) δ [ppm]: 1.89 (s, 3H), 5.10 (br s, 2H), 5.30 (br s, 2H), 5.93 (dd, J = 3.0 Hz, J = 3.0 Hz, 1H), 5.97 (br s, 1H), 6.83 (t, J = 2.5 Hz, 1H), 6.91−6.95 (m, 2H), 7.04 (d, J = 6.5 Hz, 1H), 7.10 (t, J = 6.5 Hz, 1H), 7.16−7.21 (m, 2H), 7.30 (s, 1H), 7.42−7.48 (m, 2H), 7.89 (dd, J = 7.5 Hz, J = 5.5 Hz, 1H).

*2,2,2-Trichloro-1-[10-(5′-fluoro-2-methyl-2′-trifluoromethylbiphenyl-4-carbonyl)-10,11-dihydro-5-benzo[e]pyrrolo[1,2-a][1,4]-diazepin-3-yl]ethanone (**18**; Intermediate of Reaction Step (e) in Scheme 1).* The compound was synthesized using 0.30 g (0.60 mmol) of **4a** according to the procedure for the synthesis of **15**. The obtained crude product was purified by column chromatography (*n*-hexane:EtOAc = 4:1) to yield 0.35 g (95%) of the titled product as a colorless oil. ^{1}H NMR (500 MHz, DMSO-d_6) δ [ppm]: 1.89 (s, 3H), 5.10 (br s, 2H), 5.30 (br s, 2H), 5.93 (dd, J = 3.0 Hz, J = 3.0 Hz, 1H), 5.97 (br s, 1H), 6.39 (d, J = 4.0 Hz, 1H), 6.79 (d, J = 7.0 Hz, 1H), 7.04 (d, J = 6.5 Hz, 1H), 7.10 (t, J = 6.5 Hz, 1H), 7.16−7.21 (m, 2H), 7.30 (s, 1H), 7.42−7.48 (m, 2H), 7.89 (dd, J = 7.5 Hz, J = 5.5 Hz, 1H).

*10-(5′-Fluoro-2-methyl-2′-trifluoromethylbiphenyl-4-carbonyl)-10,11-dihydro-5H-benzo[e]pyrrolo[1,2-a][1,4]diazepine-3-carboxylic Acid (**5a**).* According to the procedure for the synthesis of **5g** and using 0.35 g (0.57 mmol) of **18**, product **5a** was isolated as a white solid in 99% yield (0.29 g) and used in the next step without further purification. ^{1}H NMR (500 MHz, $CDCl_3$) δ [ppm]: 1.93 (s, 3H), 5.32 (br s, 2H), 5.98 (br s, 2H), 6.11 (d, J = 4.0 Hz, 1H), 6.79 (d, J = 7.0 Hz, 1H), 6.86 (dd, J = 8.5 Hz, J = 2.5 Hz, 1H), 6.91 (d, J = 8.0 Hz, 1H), 6.97−7.00 (m, 1H), 7.07 (t, J = 7.5 Hz, 1H), 7.09 (d, J = 4.0 Hz, 1H), 7.12−7.19 (m, 2H), 7.26 (s, 1H), 7.46 (d, J = 7.5 Hz, 1H), 7.72 (dd, J = 9.0 Hz, J = 5.5 Hz, 1H).

*10-(5′-Fluoro-2-methyl-2′-trifluoromethylbiphenyl-4-carbonyl)-10,11-dihydro-5H-benzo[e]pyrrolo[1,2-a][1,4]diazepine-3-carboxylic Acid Bis(2-hydroxyethyl) Amide (**6a**).* A mixture of 290 mg (0.57 mmol) of **5a**, 75 mg (0.72 mmol) of diethanol amine, 86 mg (0.63 mmol) of HOBt, 127 mg (0.66 mmol) of EDCI, and 0.15 mL (113 mg, 0.87 mmol) of Hünig's base in 4 mL of DMF was stirred at rt overnight. The mixture was concentrated, and the residue was diluted with 7 mL of H_2O and extracted three times with 7 mL of EtOAc. The organic layer was washed twice with 5 mL of a saturated aqueous $NaHCO_3$ solution, dried over Na_2SO_4, filtered, and concentrated to remove the solvent. Column chromatography (CH_2Cl_2:methanol = 95:5) followed by crystallization from EtOAc to remove traces of impurities afforded 190 mg (56%) of **5a** as a white solid; mp 100−107 °C. ^{1}H NMR (500 MHz, DMSO-d_6) δ [ppm]: 1.88 (s, 3H), 3.48−3.65 (m, 8H), 4.82 (t, J = 5.0 Hz, 2H), 5.25 (br s, 2H), 5.34 (br s, 2H), 6.03 (d, J = 3.0 Hz, 1H), 6.30 (d, J = 3.5 Hz, 1H), 6.87 (d, J = 6.0 Hz, 1H), 6.93 (d, J = 7.5 Hz, 1H), 7.01−7.07 (m, 2H), 7.13−7.18 (m, 2H), 7.28 (s, 1H), 7.38 (d, J = 7.0 Hz, 1H), 7.44 (td, J = 8.0 Hz, J = 2.5 Hz, 1H), 7.88 (dd, J = 9.0 Hz, J = 5.5 Hz, 1H). ^{13}C NMR (125 MHz, DMSO-d_6) δ [ppm] 19.29, 45.89, 47.03, 58. 45, 58. 56, 107.50, 110.23, 115.10 (d, J = 21.6 Hz), 118.30 (d, J = 22.1 Hz), 122.27, 123.50 (q, J = 29.9 Hz), 124.44, 124.51, 127.01, 127.36, 128.21, 128.44, 128.71, 128.75, 128.98 (m), 129.07, 129.29, 134.70, 135.07, 135.64, 138.42, 141.32, 142.03 (d, J = 7.6 Hz), 162.32, 163.76, 164.33, 169.04. LC/MS retention time: 8.94 min. MS (ESI) m/z = 596.4 $[M + H]^+$.

*Synthesis of **6b**. 2-(2-Fluoroethyl)phenyl Bromide (**1b**).* A mixture of 5 g (25 mmol) of 2-(2-hydroxyethyl)phenyl bromide and 3.5 mL (27 mmol) of DAST in 75 mL of dry CH_2Cl_2 was stirred at rt for 20 h. The reaction mixture was diluted with 150 mL of saturated aqueous $NaHCO_3$ solution and stirred for additional 30 min. The CH_2Cl_2 layer was separated, and the aqueous layer was extracted with CH_2Cl_2. The combined organic layers were dried over Na_2SO_4, filtered, and concentrated to remove the CH_2Cl_2. Purification by column chromatography (PE:EtOAc = 9:1) provided 3.2 g (63%) of **1b** as a colorless liquid. ^{1}H NMR (500 MHz, $CDCl_3$) δ [ppm]: 3.19 (dt, J = 22.5 Hz, J = 7.0 Hz, 2H), 4.66 (dt, J = 47.5 Hz, J = 6.5 Hz, 2H), 7.12 (td, J = 7.5 Hz, 2.0 Hz, 1H), 7.25−7.31 (m, 2H), 7.56 (dd, J = 7.5 Hz, J = 1.0 Hz, 1H).

*2-(2-Fluoroethyl)phenylboronic Acid (**2b**).* According to the procedure of **2g** described above, 3.0 g (15 mmol) of **1b**, 80 mL of dry THF, 7.2 mL of *n*-BuLi (2.5 M in *n*-hexane, 18 mmol), and 2.0 mL (18 mmol) of trimethyl borate reacted to give 2.0 g (79%) of the boronic acid **2b** as a clear, colorless oil. The crude product was used in the next step without any further purification.

*2′-(2-Fluoroethyl)-2-methylbiphenyl-4-carboxylic Acid Methyl Ester (**3b**).* The compound was synthesized using 136 mg (0.8 mmol) of **2b** according to the procedure for the synthesis of **3g**. The obtained crude product was purified by column chromatography (EtOAc:*n*-hexane = 1:19) to give 170 mg (78%) of compound **3b** as a colorless oil. ^{1}H NMR (500 MHz, $CDCl_3$) δ [ppm] 2.05 (s, 3H), 2.55−2.65 (m, 1H), 2.73−2.83 (m, 1H), 3.87 (s, 3H), 4.38 (t, J = 6.5 Hz, 1H), 4.47 (t, J = 6.5 Hz, 1H), 7.10 (d, J = 7.5 Hz, 1H), 7.25 (d, J = 8.0 Hz, 1H), 7.33 (td, J = 7.5 Hz, J = 1.5 Hz, 1H), 7.38 (td, J = 7.5 Hz, J = 1.5 Hz, 1H), 7.44 (d, J = 7.5 Hz, 1H), 7.83 (dd, J = 7.5 Hz, J = 1.5 Hz, 1H), 7.92 (s, 1H).

*(5H,11H-Benzo[e]pyrrolo[1,2-a][1,4]diazepin-10-yl)-[2′-(2-fluoroethyl)-2-methylbiphenyl-4-yl]methanone (**4b**).* According to the procedure described for the synthesis of **4g**, compound **3b** was hydrolyzed and 1.03 g (4.0 mmol) of the resulting carboxylic acid was used to react with **8**. The obtained crude product was purified by crystallization from EtOAc to give 1.60 g (99%) of **4b** as a colorless crystalline solid. ^{1}H NMR (500 MHz, $CDCl_3$) δ [ppm]: 1.86 (s, 3H),

DOI: 10.1021/acs.jmedchem.5b01080
J. Med. Chem. XXXX, XXX, XXX−XXX

2.41−2.51 (m, 1H), 2.62−2.72 (m, 1H), 4.23 (t, J = 6.5 Hz, 1H), 4.32 (t, J = 6.5 Hz, 1H), 5.10 (br s, 2H), 5.31 (br s, 2H), 5.93 (dd, J = 3.5 Hz, J = 2.0 Hz, 1H), 5.97 (br s, 1H), 6.84 (t, J = 2.5 Hz, 1H), 6.89−6.95 (m, 2H), 7.01 (d, J = 6.5 Hz, 1H), 7.04 (d, J = 7.5 Hz, 1H), 7.09 (t, J = 7.5 Hz, 1H), 7.18 (t, J = 7.5 Hz, 1H), 7.25−7.34 (m, 3H), 7.37 (d, J = 7.5 Hz, 1H), 7.47 (d, J = 7.5 Hz, 1H).

*2,2,2-Trichloro-1-[10-[2′-(2-fluoroethyl)-2-methylbiphenyl-4-carbonyl]-10,11-dihydro-5H-benzo[e]pyrrolo[1,2-a][1,4]diazepin-3-yl]-ethanone (**19**; Intermediate of Reaction Step (e) in Scheme 1).* The compound was synthesized from 1.6 g (3.9 mmol) of **4b** according to the procedure for the synthesis of **15**. The obtained crude product was purified by column chromatography (EtOAc:*n*-hexane = 1:4) to give 2.1 g (95%) of the titled compound as a white solid. ^{1}H NMR (500 MHz, $CDCl_3$) δ [ppm]: 1.87 (s, 3H), 2.42−2.51 (m, 1H), 2.63−2.73 (m, 1H), 4.23 (t, J = 7.0 Hz, 1H), 4.33 (t, J = 7.0 Hz, 1H), 5.31 (br s, 2H), 5.99 (br s, 2H), 6.39 (d, J = 4.0 Hz, 1H), 6.89−6.93 (m, 2H), 7.02 (dd, J = 7.5 Hz, J = 1.5 Hz, 1H), 7.04−7.12 (m, 2H), 7.18 (td; J = 7.5 Hz, J = 1.5 Hz, 1H), 7.28 (td, J = 7.5 Hz, J = 1.5 Hz, 1H), 7.30−7.35 (m, 2H), 7.37 (d, 7.5 Hz, 1H), 7.44 (dd, 7.5 Hz, J = 1.5 Hz, 1H), 7.47 (d, J = 4.5 Hz, 1H).

*10-[2′-(2-Fluoroethyl)-2-methylbiphenyl-4-carbonyl]-10,11-dihydro-5H-benzo[e]pyrrolo[1,2-a][1,4]diazepine-3-carboxylic Acid (**5b**).* The compound was synthesized using 2.1 g (3.7 mmol) of **19** according to the procedure for the synthesis of **5g**. The obtained crude product was purified by column chromatography (EtOAc:*n*-hexane = 1:4) to give 1.6 g (92%) of **5b** as a white solid; mp 184−190 °C. ^{1}H NMR (500 MHz, $CDCl_3$) δ [ppm]: 1.86 (s, 3H), 2.42−2.51 (m, 1H), 2.62−2.73 (m, 1H), 4.23 (t, J = 7.0 Hz, 1H), 4.33 (t, J = 7.0 Hz, 1H), 5.19 (br s, 2H), 5.94 (br s, 2H), 6.12 (d, J = 4.0 Hz, 1H), 6.77 (d, J = 4.0 Hz, 1H), 6.86 (d, J = 7.5 Hz, 1H), 6.90 (d, J = 8.0 Hz, 1H), 7.00−7.06 (m, 3H), 7.14 (t, J = 7.0 Hz, 1H), 7.25−7.38 (m, 5H), 12.34 (br s, 1H).

*10-[2′-(2-Fluoroethyl)-2-methylbiphenyl-4-carbonyl]-10,11-dihydro-5H-benzo[e]pyrrolo[1,2-a][1,4]diazepine-3-carboxylic Acid Bis-(2-hydroxyethyl)amide (**6b**).* To an ice-cooled solution of 100 mg (0.21 mmol) of **5b** and 0.05 mL (0.42 mmol) of *N*-methylmorpholine in 2 mL of DMF, 91.4 mg of COMU (0.21 mmol) was added. After stirring for 10 min, a solution of 0.02 mL (0.21 mmol) of diethanolamine in 1 mL of DMF was added dropwise. The resultant bright-yellow solution was stirred for additional 30 min before the cooling bath was removed. The mixture was allowed to warm to rt overnight. The complete consumption of the starting material was confirmed by TLC (CH_2Cl_2:methanol = 95:5), and the reaction mixture was diluted with 5 mL of EtOAc. The organic layer was subsequently washed with aqueous $KHSO_4$ (5 wt %), aqueous $NaHCO_3$ (5 wt %), and brine and dried over Na_2SO_4. After filtration and removal of the solvent under reduced pressure the crude product was purified by column chromatography (CH_2Cl_2:methanol = 97:3) to give 73 mg (61%) of **6b** as a white solid; mp 90−94 °C. ^{1}H NMR (500 MHz, DMSO-d_6) δ [ppm]: 1.86 (s, 3H), 2.43−2.52 (m, 1H), 2.62−2.72 (m, 1H), 3.56 (br s, 8H), 4.23 (t, J = 6.5 Hz, 1H), 4.32 (t, J = 6.5 Hz, 1H), 4.83 (t, J = 5.0 Hz, 2H), 5.20 (br s, 2H), 5.34 (br s, 2H), 6.03 (d, J = 3.5 Hz, 1H), 6.30 (d, J = 3.5 Hz, 1H), 6.85−6.91 (m, 2H), 7.00−7.07 (m, 3H), 7.14 (t, J = 7.5 Hz, 1H), 7.25−7.29 (m, 2H), 7.32 (td, J = 1.5 Hz, J = 8.0 Hz, 1H), 7.37 (d, J = 7.5 Hz, 2H). ^{13}C NMR (125 MHz, DMSO-d_6) δ [ppm]: 19.32, 33.10 (d, J = 20 Hz), 45.83, 47.03, 58.55, 82.76 (d, J = 166 Hz), 107.50, 110.22, 125.11, 126.48, 126.97, 127.35, 127.55, 128.38, 128.51, 128.73, 128.91, 129.11, 129.60, 129.66, 134.05, 134.10, 134.77, 134.92, 140.26, 141.46, 141.62, 163.75, 169.23. LC/MS retention time: 8.61 min. MS (ESI) m/z = 556.2 $[M + H]^+$.

*Synthesis of **6c**. 10-(2-Methyl-2′-trifluoromethylbiphenyl-4-carbonyl)-10,11-dihydro-5H-benzo[e]pyrrolo[1,2-a][1,4]diazepine-3-carboxylic Acid (2-Fluoroethyl)-(2-hydroxyethyl)amide (**6c**).* To a solution of 50 mg (0.09 mmol) of **6** (synthesized according to literature[26]) in 0.4 mL of dry CH_2Cl_2, 0.01 mL (0.1 mmol) of DAST was added. The mixture was stirred at rt overnight. TLC analysis confirmed the complete consumption of the starting material. Purification via column chromatography (CH_2Cl_2:methanol = 95:5) provided 32 mg (64%) of **6c** as a white solid; mp 82−85 °C. ^{1}H NMR (500 MHz, DMSO-d_6) δ [ppm]: 1.85 (s, 3H), 2.83 (t, J = 5.0 Hz, 1H), 2.87−2.91 (m, 3H), 4.26 (t, J = 5.5 Hz, 2H), 4.46 (dt, J = 47.5 Hz, J = 5.0 Hz, 2H), 5.20 (br s, 2H), 5.93 (br s, 2H), 6.16 (d, J = 3.5 Hz, 1H), 6.85 (d, J = 3.5 Hz, 1H), 6.87 (d, J = 8.0 Hz, 1H), 6.91 (d, J = 8.0 Hz, 1H), 7.00−7.08 (m, 2H), 7.15 (td, J = 7.5 Hz, J = 1.0 Hz, 1H), 7.22 (d, J = 7.5 Hz, 1H), 7.27 (s, 1H), 7.37 (dd, J = 7.5 Hz, J = 1.0 Hz, 1H), 7.60 (t, J = 7.5 Hz, 1H), 7.69 (t, J = 7.5 Hz, 1H), 7.80 (d, J = 8.0 Hz, 1H). ^{13}C NMR (125 MHz, DMSO-d_6) δ [ppm]: 19.39, 45.99 (br s), 46.21, 47.39, 48.63 (d, J = 20 Hz), 63.12, 83.35 (d, J = 162 Hz), 109.25, 117.80, 121.46, 121.53, 123.73 (q, J = 272 Hz), 124.56, 125.90 (q, J = 5 Hz), 126.87 (q, J = 29 Hz), 127.15, 128.13, 128.35, 128.47, 128.59, 129.29, 130.37, 131.14, 132.19, 134.08, 134.87, 135.10, 138.86 (q, J = 1.5 Hz), 139.82, 141.15, 160.37, 169.17. LC/MS retention time: 9.39 min. MS (ESI) m/z = 580.1 $[M + H]^+$.

*Synthesis of **6d**−**6f**. 10-(2-Methyl-2′-trifluoromethylbiphenyl-4-carbonyl)-10,11-dihydro-5H-benzo[e]pyrrolo[1,2-a][1,4]diazepine-3-carboxylic Acid (**5c**).*[26] Compound **5c** was synthesized in five steps starting from 5.2 g (27 mmol) of commercially available **2c** and 6 g (26 mmol) of methyl 4-bromo-3-methylbenzoate according to the published procedure for the synthesis of **6**.[26] The obtained crude product was purified by crystallization from EtOAc to give 6.5 g (50%) of **5c** as a white solid; mp 230−234 °C. ^{1}H NMR (500 MHz, DMSO-d_6) δ [ppm]: 1.85 (3H, s), 5.19 (br s, 2H), 5.95 (br s, 2H), 6.12 (d, J = 4.0 Hz, 1H), 6.77 (d, J = 4.0 Hz, 1H), 6.87 (d, J = 7.5 Hz, 1H), 6.91 (d, J = 7.5 Hz, 1H), 7.01−7.07 (m, 2H), 7.15 (t, J = 7.5 Hz, 1H), 7.22 (d, J = 8.0 Hz, 1H), 7.27 (s, 1H), 7.34 (d, J = 7.0 Hz, 1H), 7.60 (t, J = 7.5 Hz, 1H), 7.69 (t, J = 8.0 Hz, 1H), 7.80 (d, J = 7.5 Hz, 1H), 12.33 (br s, 1H).

*10-(2-Methyl-2′-trifluoromethylbiphenyl-4-carbonyl)-10,11-dihydro-5H-benzo[e]pyrrolo[1,2-a][1,4]diazepine-3-carboxylic Acid (2-Fluoroethyl)amide (**6d**).* To a solution of 200 mg (0.41 mmol) of **5c** in 3.5 mL of THF, a mixture of 0.2 mL (0.98 mmol) Hünig's base, 66 mg (0.66 mmol) of 2-fluoroethylamine hydrochloride, and 170 mg (0.53 mmol) of TBTU was added. The mixture was stirred at rt overnight and diluted with 5 mL of a 0.5 M aqueous $NaHCO_3$ solution followed by extraction with EtOAc. The combined organic layers were dried over Na_2SO_4, filtered, and concentrated in vacuum. Purification by column chromatography (*n*-hexane:EtOAc = 2:1) afforded 176 mg (81%) of **6d** as a white solid; mp 197−200 °C. ^{1}H NMR (500 MHz, DMSO-d_6) δ [ppm]: 1.84 (s, 3H), 3.52 (dq, J = 30.0 Hz, J = 5.5 Hz, 2H), 4.52 (dt, J = 47.5 Hz, J = 5.0 Hz, 2H), 5.16 (br s, 2H), 5.94 (br s, 2H), 6.07 (d, J = 4.0 Hz, 1H), 6.72 (d, J = 4.0 Hz, 1H), 6.83 (d, J = 7.5 Hz, 1H), 6.90 (d, J = 7.5 Hz, 1H), 6.98−7.03 (m, 2H), 7.12 (td, J = 7.5 Hz, J = 1.0 Hz, 1H), 7.22 (d, J = 7.5 Hz, 1H), 7.26 (s, 1H), 7.32 (dd, J = 7.5 Hz, J = 1.0 Hz, 1H), 7.60 (t, J = 7.5 Hz, 1H), 7.69 (t, J = 7.5 Hz, 1H), 7.80 (d, J = 7.5 Hz, 1H). ^{13}C NMR (125 MHz, DMSO-d_6) δ [ppm]: 19.38, 45.89, 46.14 (br s), 64.79, 82.21 (d, J = 164.8 Hz), 108.45, 112.35, 123.74 (q, J = 272.4 Hz), 124.56, 125.75, 125.89 (q, J = 4.9 Hz), 126.89 (q, J = 29.3 Hz), 126.92, 128.11, 128.23, 128.35, 129.29, 131.09, 131.15, 132.17, 135.07, 135.31, 135.37, 138.90 (q, J = 1.6 Hz), 139.73, 141.00, 161.49, 169.16. LC/MS retention time: 10.16 min. MS (ESI) m/z = 536.1 $[M + H]^+$.

*10-(2-Methyl-2′-trifluoromethylbiphenyl-4-carbonyl)-10,11-dihydro-5H-benzo[e]pyrrolo[1,2-a][1,4]diazepine-3-carboxylic Acid (2-Fluoroethyl)methyl Amide (**6e**).* To a stirred solution of 164 mg (0.3 mmol) of **6d** in 0.3 mL of DMF, 44 mg (1.8 mmol, 60 wt % in mineral oil) of NaH was added followed by the addition of 0.11 mL (1.8 mmol) of methyl iodide. After stirring for 1 h at rt, the complete consumption of the reaction was confirmed by TLC analysis (*n*-hexane:EtOAc = 3:2). The mixture was quenched with 1 mL of H_2O followed by extraction with EtOAc. The combined organic layers were dried over Na_2SO_4, filtered, and concentrated in vacuum. The crude product was purified by column chromatography (*n*-hexane:EtOAc = 3:1) to obtain 80 mg (47%) of **6e** as a white solid; mp 165−168 °C. ^{1}H NMR (500 MHz, DMSO-d_6) δ [ppm]: 1.84 (s, 3H), 3.11 (br s, 3H), 3.80 (dt, J = 26.5 Hz, J = 5.0 Hz, 2H), 4.65 (dt, J = 47.5 Hz, J = 5.0 Hz, 2H), 5.17 (br s, 2H), 5.41 (br s, 2H), 6.07 (d, J = 3.5 Hz, 1H), 6.32 (d, J = 3.5 Hz, 1H), 6.86−6.92 (m, 2H), 7.00−7.08 (m, 2H), 7.15 (t, J = 7.5 Hz, 1H), 7.22 (d, J = 8.0 Hz, 1H), 7.26 (s, 1H), 7.37 (d, J = 7.0 Hz, 1H), 7.59 (t, J = 8.0 Hz, 1H), 7.68 (t, J = 7.5 Hz, 1H), 7.80 (d,

DOI: 10.1021/acs.jmedchem.5b01080
J. Med. Chem. XXXX, XXX, XXX−XXX

J = 8.0 Hz, 1H). ^{13}C NMR (125 MHz, DMSO-d_6) δ [ppm]: 19.48, 45.88, 46.96, 80.87, 82.18, 107.72, 111.59, 120.46, 122.64, 124.51, 124.82, 125.87 (q, J = 5.0 Hz, 1C), 126.19, 126.54, 126.77, 126.99, 127.23, 128.11, 128.35, 128.45, 128.68, 129.10, 129.24, 129.66, 131.14, 132.17, 134.70, 135.08, 135.22, 138.87 (q), 139.78, 141.32, 163.28, 169.14. LC/MS retention time: 10.33 min. MS (ESI) m/z = 550.1 [M + H]$^+$.

*[2′-(2-Fluoroethyl)-2-methylbiphenyl-4-yl]-[3-(morpholino-4-carbonyl)-5H,11H-benzo[e]pyrrolo[1,2-a][1,4]diazepin-10-yl]-methanone (**6f**).* A mixture of 150 mg (0.32 mmol) of **5b**, 183 mg (0.48 mmol) of 1-bis(dimethylamino)methylene-1*H*-1,2,3-triazolo-[4,5-*b*]pyridinium-3-oxid hexafluorophosphate, (HATU) 0.32 mL (1.9 mmol) of Hünig's base, and 0.11 mL (1.28 mmol) of morpholine dissolved in 15 mL of DMF was stirred at rt overnight. The mixture was concentrated, and the residue was diluted with 7 mL of H_2O and extracted three times with 7 mL of EtOAc. The organic layer was washed twice with 5 mL of a saturated aqueous $NaHCO_3$ solution, dried over Na_2SO_4, filtered, and concentrated to remove the solvent. Column chromatography (*n*-hexane:EtOAc = 1:1) afforded 158 mg (92%) of **6f** as a white solid; mp 190−193 °C. ^{1}H NMR (500 MHz, DMSO-d_6) δ [ppm]: 1.86 (s, 3H), 2.42−2.52 (m, 1H), 2.62−2.71 (m, 1H), 3.63 (br s, 8H), 4.28 (dt, J = 47.0 Hz, J = 6.5 Hz, 2H), 5.17 (br s, 2H), 5.43 (br s, 2H), 6.08 (d, J = 4.0 Hz, 1H), 6.28 (d, J = 4.0 Hz, 1H), 6.86 (d, J = 7.5 Hz, 1H), 6.90 (d, J = 7.5 Hz, 1H), 7.00−7.07 (m, 3H), 7.15 (td, J = 7.5 Hz, J = 1.0 Hz, 1H), 7.25−7.29 (m, 2H), 7.32 (td, J = 7.5 Hz, J = 1.0 Hz, 1H), 7.37 (d, J = 7.5 Hz, 1H), 7.42 (dd, J = 7.5 Hz, J = 1.0 Hz, 1H). ^{13}C NMR (125 MHz, DMSO-d_6) δ [ppm]: 19.32, 33.1 (d, J = 20.4 Hz), 38.13, 45.84 (br s), 46.91, 66.14, 82.75 (d, J = 165.7 Hz), 107.86, 111.65, 125.12, 125.64, 126.47, 127.00, 127.55, 128.42, 128.50, 128.71, 128.90, 129.16, 129.62, 129.65, 129.95, 134.06 (d, J = 6.5 Hz), 134.74, 134.80, 134.93, 140.25, 141.39, 141.64, 161.73, 169.23. LC/MS retention time: 9.81 min. MS (ESI) m/z = 538.2 [M + H]$^+$.

*Synthesis of **12a** and **12b**. 2′-(2-Fluoroethyl)-2-methylbiphenyl-4-carboxylic Acid (**9**).* The compound was synthesized using 1.17 g (4.3 mmol) of **3b** according to the procedure for the synthesis of **4g**. After workup, 1.05 g (95%) of a white solid was obtained and used in the next step without any further purification; mp 128−130 °C. ^{1}H NMR (500 MHz, DMSO-d_6) δ [ppm]: 2.04 (s, 3H), 2.56−2.66 (m, 1H), 2.74−2.84 (m, 1H), 4.37 (t, J = 6.5 Hz, 1H), 4.47 (t, J = 6.5 Hz, 1H), 7.10 (d, J = 7.5 Hz, 1H), 7.22 (d, J = 8.0 Hz, 1H), 7.32 (td, J = 7.5 Hz, J = 1.5 Hz, 1H), 7.38 (td, J = 7.5 Hz, J = 1.5 Hz, 1H), 7.44 (d, J = 7.5 Hz, 1H), 7.82 (dd, J = 7.5 Hz, J = 1.5 Hz, 1H), 7.90 (s, 1H).

*(3,4-Dihydro-1H-pyrrolo[1,2-a]pyrazin-2-yl)-[2′-(2-fluoroethyl)-2-methylbiphenyl-4-yl]methanone (**10**).* A solution of 1.6 g (6.2 mmol) of **9** in 10 mL of thionyl chloride was refluxed under argon atmosphere for 1 h. The excess of thionyl chloride was removed under vacuum, and the residue was treated three times with 5 mL of toluene followed by removal of the solvent. The resultant acid chloride was dissolved in 10 mL of CH_2Cl_2 and added dropwise to an ice-cold solution of 0.85 g (7.0 mmol) of 1,2,3,4-tetrahydro-pyrrolo[1,2-*a*]pyrazine (synthesized according to procedures described[31]) and 2.5 mL (13.6 mmol) of Hünig's base in 30 mL of CH_2Cl_2. The cooling bath was removed and the mixture stirred for 4 h at rt. After hydrolysis of the reaction with 50 mL of H_2O, the aqueous layer was extracted three times with CH_2Cl_2. The combined organic layers were washed with an aqueous solution of $NaHCO_3$, dried over Na_2SO_4, filtered, and concentrated. The crude product was purified by column chromatography (EtOAc:*n*-hexane = 1:9) to obtain 1.5 g (67%) of **10** as a white foam; mp 50−54 °C. ^{1}H NMR (500 MHz, $CDCl_3$) δ [ppm]: 2.08 (s, 3H), 2.68−2.78 (m, 1H), 2.84−2.91 (m, 1H), 3.90 (br s, 2H), 4.10 (br s, 2H), 4.43 (dt, J = 47.5 Hz, J = 6.5 Hz, 2H), 4.80 (br s, 2H), 5.90 (br s, 1H), 6.19−6.25 (m, 1H), 6.63 (t, 1H), 7.11 (d, J = 7.5 Hz, 1H), 7.17 (d, J = 8 Hz, 1H), 7.29−7.32 (m, 2H), 7.36−7.39 (m, 3H).

*2,2,2-Trichloro-1-[2-[2′-(2-fluoroethyl)-2-methylbiphenyl-4-carbonyl]-1,2,3,4-tetrahydropyrrolo[1,2-a]pyrazin-6-yl]ethanone (**20**; Intermediate of Reaction Step (e) in Scheme 2).* The compound was synthesized using 1.4 g (3.9 mmol) of **10** according to the procedure for the synthesis of **15**. The obtained crude product was purified by column chromatography (*n*-hexane:EtOAc = 2:1) to yield 1.5 g (76%) of the titled product as a yellowish foam; mp 87−92 °C. ^{1}H NMR (500 MHz, DMSO-d_6) δ [ppm]: 2.04 (s, 3H), 2.61−2.72 (m, 1H), 2.77−2.88 (m, 1H), 4.88 (br s, 2H), 4.45 (dt, J = 47.5 Hz, J = 6.5 Hz, 2H), 4.46 (t, J = 5.5 Hz, 2H), 4.91 (br s, 2H), 6.34 (br s, 1H), 7.13 (dd, J = 7.5 Hz, J = 1.0 Hz, 1H), 7.21 (d, J = 7.5 Hz, 1H), 7.33 (td, J = 7.5 Hz, J = 1.0 Hz, 1H), 7.37−7.41 (m, 2H), 7.44−7.51 (m, 3H).

*2-[2′-(2-Fluoroethyl)-2-methylbiphenyl-4-carbonyl]-1,2,3,4-tetrahydropyrrolo[1,2-a]pyrazine-6-carboxylic Acid (**21**; Intermediate of Reaction Step (f) in Scheme 2).* According to the procedure for the synthesis of **5g** and using 1.2 g (2.4 mmol) of **20** in 50 mL of acetone and 10 mL (2.5 M) of an aqueous NaOH solution, 900 mg (91%) of the product was isolated as a white solid and used in the next step without further purification. ^{1}H NMR (500 MHz, DMSO-d_6)) δ [ppm]: 2.03 (s, 3H), 2.60−2.71 (m, 1H), 2.76−2.87 (m, 1H), 3.83 (br s, 2H), 4.41 (t, J = 7.0 Hz, 1H), 4.51 (t, J = 7.0 Hz, 1H), 4.53 (br s, 2H), 4.80 (br s, 2H), 6.05 (br s, 1H), 6.83 (br s, 1H), 7.13 (dd, J = 7.5 Hz, J = 1.5 Hz, 1H), 7.19 (d, J = 7.5 Hz, 1H), 7.33 (td, J = 7.5 Hz, 1.5 Hz, 1H), 7.35−7.40 (m, 2H), 7.44−7.46 (m, 2H), 12.07 (br s, 1H).

*2-[2′-(2-Fluoroethyl)-2-methylbiphenyl-4-carbonyl]-1,2,3,4-tetrahydropyrrolo[1,2-a]pyrazine-6-carboxylic Acid Bis(2-hydroxyethyl)amide (**12a**).* The compound was synthesized using 110 mg (0.28 mmol) of **21** and 52 mg (0.5 mmol) of diethanolamine according to the procedure for the synthesis of **6b**. The obtained crude product was purified by column chromatography (CH_2Cl_2:methanol = 97:3) to yield 25 mg (18%) of **12a** as a white foam; mp 72−75 °C. ^{1}H NMR (500 MHz, DMSO-d_6)) δ [ppm]: 2.03 (s, 3H), 2.60−2.71 (m, 1H), 2.76−2.87 (m, 1H), 3.55 (br s, 8H), 3.70−4.00 (br s, 2H), 4.12 (t, J = 5.0 Hz, 2H), 4.46 (dt, J = 47.0 Hz, 6.5 Hz, 2H), 4.78 (br s, 4H), 5.96 (br s, 1H), 6.47 (br s, 1H), 7.13 (dd, J = 7.5 Hz, J = 1.5 Hz, 1H), 7.19 (d, J = 7.5 Hz, 1H), 7.31−7.40 (m, 3H), 7.45 (br d, J = 7.5 Hz, 2H). ^{13}C NMR (125 MHz, DMSO-d_6) δ [ppm]: 19.44, 30.57, 33.14 (d, J = 20.1 Hz), 37.85, 46.87, 54.79, 65.78, 66.11, 83.05 (d, J = 165.5 Hz), 103.34 (br s), 123.07, 123.66, 124.26, 124.30, 126.49, 127.63, 128.52, 128.63, 129.04, 129.35, 129.48, 134.36 (d, J = 6.0 Hz), 135.75, 140.42, 161.52, 162.38. LC/MS retention time: 7.87 min. MS (ESI) m/z = 494.2 [M + H]$^+$.

*2-[2′-(2-Fluoroethyl)-2-methylbiphenyl-4-carbonyl]-1,2,3,4-tetrahydropyrrolo[1,2-a]pyrazine-6-carboxylic Acid (2-Hydroxyethyl)methyl Amide (**12b**).* The compound was synthesized using 110 mg (0.28 mmol) of **21** and 38 mg (0.5 mmol) of 2-methylaminoethanol according to the procedure for the synthesis of **6b**. The obtained crude product was purified by column chromatography (CH_2Cl_2:methanol = 97:3) to yield 50 mg (39%) of **12b** as a white solid; mp 125−129 °C. ^{1}H NMR (500 MHz, DMSO-d_6) δ [ppm]: 2.03 (s, 3H), 2.60−2.71 (m, 1H), 2.76−2.87 (m, 1H), 3.06 (br s, 3H), 3.53−3.58 (m, 4H), 3.78 (br s, 2H), 4.17 (t, J = 5.5 Hz, 2H), 4.46 (dt, J = 47.0 Hz, 6.5 Hz, 2H), 4.77 (br s, 3H), 5.97 (br s, 1H), 6.47 (br s, 1H), 7.13 (dd, J = 7.5 Hz, J = 1.5 Hz, 1H), 7.19 (d, J = 7.5 Hz, 1H), 7.31−7.40 (m, 3H), 7.44 (d, J = 7.5 Hz, 2H). ^{13}C NMR (125 MHz, DMSO-d_6) δ [ppm]: 19.45, 33.14 (d, J = 20.4 Hz), 44.05 (br s), 44.89 (br s), 54.79, 58.32, 83.05 (d, J = 165.5 Hz), 103.11, 112.23, 124.12, 124.25, 126.48, 127.62, 127.99, 128.50, 129.14, 129.34, 129.47, 134.36 (d, J = 6.0 Hz), 135.74, 140.42, 141.94, 162.90 (br s), 169.33 (br s). LC/MS retention time: 8.37 min. MS (ESI) m/z = 464.2 [M + H]$^+$.

*Synthesis of **12c**. 4-[2-[2′-(2-Fluoroethyl)-2-methylbiphenyl-4-carbonyl]-1,2,3,4-tetrahydropyrrolo[1,2-a]pyrazine-6-carbonyl]-piperazine-1-carboxylic Acid tert-Butyl Ester (**22**; Intermediate of Reaction Step (g) in Scheme 2).* The compound was synthesized using 200 mg (0.5 mmol) of **21** and 170 mg (0.9 mmol) of 1-Boc-piperazine according to the procedure for the synthesis of **6b**. The obtained crude product was purified by column chromatography (*n*-hexane:EtOAc = 2:3) to yield 170 mg (59%) of the titled product as a white solid; mp 95−98 °C. ^{1}H NMR (500 MHz, DMSO-d_6) δ [ppm]: 1.42 (s, 9H), 2.02 (s, 3H), 2.60−2.68 (m, 1H), 2.76−2.87 (m, 1H), 3.37 (br s, 4H), 3.61 (br s, 4H), 3.78 (br s, 2H), 4.17 (dd, J = 5.0 Hz, J = 5.0 Hz, 2H) 4.41 (t, J = 6.5 Hz, 1H), 4.50 (t, J = 6.5 Hz, 1H), 4.78 (br s, 2H), 6.02 (br s, 1H), 6.42 (br s, 1H), 7.12 (dd, J = 7.5 Hz, J = 1.5 Hz, 1H), 7.20 (d, J = 7.5 Hz, 1H), 7.30−7.38 (m, 3H), 7.45 (d, J = 7.5 Hz, 2H).

DOI: 10.1021/acs.jmedchem.5b01080
J. Med. Chem. XXXX, XXX, XXX−XXX

*[2′-(2-Fluoroethyl)-2-methylbiphenyl-4-yl]-[6-(piperazine-1-carbonyl)-3,4-dihydro-1H-pyrrolo[1,2-a]pyrazin-2-yl]methanone (**12c**).* To an ice-cooled solution of 170 mg (0.3 mmol) of **22** in 5 mL of CH_2Cl_2, trifluoroacetic acid was added (0.6 mL, 0.8 mmol) under argon atmosphere. After stirring at rt for 2 h, the mixture was diluted with a saturated aqueous $NaHCO_3$ solution. The aqueous layer was extracted several times with CH_2Cl_2, the resultant organic layer washed with brine and dried over Na_2SO_4. After filtration, the solvent was removed under reduced pressure and the residue was dried in vacuum to give 120 mg (84%) of **12c** as a white solid; mp 125−130 °C. ^{1}H NMR (500 MHz, DMSO-d_6) δ [ppm]: 2.03 (s, 3H), 2.60−2.67 (m, 1H), 2.69 (dd, J = 5.0 Hz, J = 5.0 Hz, 4H), 2.76−2.87 (m, 1H), 3.55 (dd, J = 5.0 Hz, J = 5.0 Hz, 4H), 3.78 (br s, 2H), 4.17 (dd, J = 5.0 Hz, J = 5.0 Hz, 2H) 4.41 (t, J = 6.5 Hz, 1H), 4.50 (t, J = 6.5 Hz, 1H), 4.78 (br s, 2H), 5.99 (br s, 1H), 6.35 (br s, 1H), 7.13 (dd, J = 7.5 Hz, J = 1.5 Hz, 1H), 7.19 (d, J = 7.5 Hz, 1H), 7.31−7.39 (m, 3H), 7.44 (d, J = 7.5 Hz, 2H). ^{13}C NMR (125 MHz, DMSO-d_6) δ [ppm]: 19.44, 33.42 (d, J = 20.4 Hz), 43.94 (brs), 44.89 (brs), 45.31 (brs), 45.46, 83.05 (d, J = 165.1 Hz), 103.25 (brs), 112.11, 123.49, 124.27, 126.48, 127.62, 128.29 (brs), 128.53, 129.13, 129.35, 129.48, 134.36 (d, J = 6 Hz), 135.75, 140.41, 141.96, 161,41, 169.34 (brs). LC/MS retention time: 7.44 min. MS (ESI) m/z = 389.3 $[M - C_4H_9N_2]^+$, 475.2 $[M + H]^+$.

*Synthesis of **12d**. 4-([2-[2′-(2-Fluoroethyl)-2-methylbiphenyl-4-carbonyl]-1,2,3,4-tetrahydropyrrolo[1,2-a]pyrazine-6-carbonyl]-amino)piperidine-1-carboxylic Acid tert-Butyl Ester (**23**; Intermediate of Reaction Step (g) in Scheme 2).* The compound was synthesized using 200 mg (0.5 mmol) of **21** and 213 mg (0.9 mmol) of 4-amino-1-Boc-piperidine according to the procedure for the synthesis of **6b**. The obtained crude product was purified by column chromatography (*n*-hexane:EtOAc = 1:2) to yield 112 mg (38%) of the titled product as a yellow solid. ^{1}H NMR (500 MHz, DMSO-d_6) δ [ppm] 1.44 (s, 9H), 1.55−1.65 (m, 2H), 1.85−1.89 (m, 2H), 1.96 (s, 3H), 2.44−2.54 (m, 1H), 2.61−2.70 (m, 1H), 3.56 (br s, 4H), 3.71−3.85 (br s, 2H), 3.81−3.90 (m, 1H), 4.38−4.41 (m, 3H), 4.50 (t, J = 6.5 Hz, 1H), 4.75 (br s, 2H), 6.03 (d, J = 3.5 Hz, 1H), 6.30 (d, J = 3.5 Hz, 1H), 7.14 (dd, J = 7.5 Hz, J = 1.5 Hz, 1H), 7.18 (d, J = 7.5 Hz, 1H), 7.30−7.40 (m, 3H), 7.40−7.45 (m, 2H), 7.84 (d, J = 7.5 Hz, 1H). ^{13}C NMR (125 MHz, DMSO-d_6) δ [ppm] 19.32, 33.10 (d, J = 20 Hz), 45.83, 47.03, 58.55, 82.76 (d, J = 166 Hz), 107.50, 110.22, 125.11, 126.48, 126.97, 127.35, 127.55, 128.38, 128.51, 128.73, 128.91, 129.11, 129.60, 129.66, 134.05, 134.10, 134.77, 134.92, 140.26, 141.46, 141.62, 163.75, 169.23.

*2-[2′-(2-Fluoroethyl)-2-methylbiphenyl-4-carbonyl]-1,2,3,4-tetrahydropyrrolo[1,2-a]pyrazine-6-carboxylic Acid Piperidin-4-yl Amide (**12d**).* To a stirred solution of 112 mg (0.2 mmol) of **23** in 5 mL of CH_2Cl_2, 0.5 mL (0.7 mmol) of trifluoroacetic acid was added under argon atmosphere. After stirring for 2.5 h at rt, the complete consumption of the reaction was confirmed by TLC analysis (CH_2Cl_2:methanol = 9:1) and the mixture was diluted with a saturated aqueous $NaHCO_3$ solution. The aqueous layer was extracted several times with EtOAc, and the resultant organic layer washed with brine and dried over Na_2SO_4. After filtration, the solvent was removed under reduced pressure and the residue treated with diethyl ether. The precipitate was filtered and dried in vacuum to give 70 mg (71%) of **12d** as a yellow solid; mp 119−123 °C. ^{1}H NMR (500 MHz, DMSO-d_6) δ [ppm]: 1.53−1.61 (m, 2H), 1.82−1.86 (m, 2H), 2.03 (s, 3H), 2.60−2.71 (m, 1H), 2.76−2.87 (m, 3H), 3.18 (d, J = 13.0 Hz, 2H), 3.70−3.93 (m, 3H), 4.39−4.43 (m, 3H), 4.51 (t, J = 6.5 Hz, 1H), 4.77 (br s, 2H), 5.98 (br s, 1H), 6.88 (br s, 1H), 7.13 (dd, J = 7.5 Hz, J = 1.5 Hz, 1H), 7.19 (d, J = 7.5 Hz, 1H), 7.31−7.40 (m, 3H), 7.42−7.46 (m, 2H), 7.85 (d, J = 7.5 Hz, 1H). ^{13}C NMR (125 MHz, DMSO-d_6) δ [ppm]: 19.47, 28.46, 33.17 (d, J = 20.3 Hz), 42.25, 43.61, 44.69 (br s), 45.47, 83.08 (d, 165.1 Hz), 103.65 (br s), 112.53, 124.18, 124.28, 126.51, 127.66, 128.53, 129.16, 129.38, 129.50. 134.38 (d, J = 5.8 Hz), 135.77, 140.44, 142.00, 160.49, 169.33. LC/MS retention time: 7.57 min. MS (ESI) m/z = 489.2 $[M + H]^+$.

*Synthesis of **13a** and **13b**. 1-[2′-(2-Fluoroethyl)-2-methylbiphenyl-4-carbonyl]-piperidin-4-one (**24**; Intermediate of Reaction Step (a) in Scheme 2).* The compound was synthesized using 500 mg (2.0 mmol) of **9** and 338 mg (2.2 mmol) of 4-piperidone monohydrate hydrogen chloride according to the procedure for the synthesis of **6b** to give 600 mg (88%) of the titled compound. The obtained crude product was used for the next step without further purification. ^{1}H NMR (500 MHz, $CDCl_3$) δ [ppm]: 2.08 (s, 3H), 2.54 (br s, 4H), 2.67−2.78 (m, 1H), 2.80−2.90 (m, 1H), 3.94 (br s, 4H), 4.42 (dt, J = 47.0 Hz, J = 6.5 Hz, 2H), 7.09 (dd, J = 7.5 Hz, J = 1.0 Hz, 1H), 7.18 (d, J = 7.5 Hz, 1H), 7.27−7.40 (m, 5H). ^{13}C NMR (125 MHz, $CDCl_3$) δ [ppm] 19.96, 33.82 (d, J = 20.6 Hz), 41.23 (br s), 46.51 (br s), 83.31 (d, J = 168.5 Hz), 124.07, 126.69, 127.86, 128.71, 129.50, 129.70, 129.75, 134.19, 134.41 (d, J = 6.6 Hz), 136.79, 140.67, 142.99, 170.88, 206.62.

*{4-[Bis(2-hydroxyethyl)amino]-piperidin-1-yl]-[2′-(2-fluoroethyl)-2-methylbiphenyl-4-yl]methanone (**13a**) and (2′-(2-Fluoroethyl)-2-methyl-[1,1′-biphenyl]-4-yl)(4-hydroxypiperidin-1-yl)methanone (**13b**).* To a stirred solution of 370 mg (1.1 mmol) of **24** and 130 mg (1.2 mmol) of diethanolamine in 4 mL dichloroethane, $Na(OAc)_3BH$ (340 mg, 1.6 mmol) and acetic acid (72 mg, 1.2 mmol) were added. The mixture was stirred at rt overnight and diluted with 10 mL of a saturated aqueous $NaHCO_3$ solution. The aqueous layer was extracted with CH_2Cl_2 and the organic layer dried over Na_2SO_4. After filtration and removal of the solvent in vacuum, the crude product was purified by column chromatography (CH_2Cl_2:methanol:triethyl amine = 90:10:1) to give both compounds as white solids in a ratio of 1:3; 30 mg (6%) of **13a** (R_f = 0.3; CH_2Cl_2:methanol = 95:5) and 90 mg (24%) of **13b** (R_f = 0.7; CH_2Cl_2:methanol = 95:5).

13a: mp 55−60 °C. ^{1}H NMR (500 MHz, DMSO-d_6) δ [ppm] 1.35−1.45 (m, 2H), 1.65−1.85 (m, 2H), 2.01 (s, 3H), 2.57−2.69 (m, 5H), 2.75−2.86 (m, 3H), 3.05 (br s, 2H), 3.40 (br s, 4H), 3.72 (br s, 1H), 4.36 (br s, 1H), 4.45 (dt, 47.5 Hz, J = 6.5 Hz, 2H), 4.55 (br s, 1H), 7.12 (dd, J = 7.5 Hz, J = 1.5 Hz, 1H), 7.15 (d, J = 7.5 Hz, 1H), 7.25 (d, J = 7.5 Hz, 1H), 7.31 (dd, J = 7.5 Hz, J = 1.5 Hz, 1H), 7.33 (s, 1H), 7.37 (td, J = 7.5, J = 1.5 Hz, 1H), 7.44 (d, J = 7.5 Hz, 1H). ^{13}C NMR (125 MHz, DMSO-d_6) δ [ppm]: 19.46, 33.13 (d, J = 20 Hz), 40.97 (br s), 46.55 (br s), 52.98, 54.79, 59.10, 59.50 (br s), 83.04 (d, J = 165 Hz), 123.84, 126.47, 127.57, 128.13, 129.17 (d, J = 4.9 Hz), 129.44, 134.31, 134.36, 135.27, 135.55, 140.50, 141.34, 168.66. LC/MS retention time: 6.94 min. MS (ESI) m/z = 429.2 $[M + H]^+$.

13b: mp 132−134 °C. ^{1}H NMR (500 MHz, DMSO-d_6) δ [ppm] 1.35−1.45 (m, 2H), 1.65−1.85 (m, 2H), 2.01 (s, 3H), 2.57−2.69 (m, 1H), 2.75−2.85 (m, 1H), 3.21 (br s, 2H), 3.57 (br s, 1H), 3.72−3.78 (m, 1H), 4.03 (br s, 1H), 4.45 (dt, J = 47.0 Hz, J = 6.5 Hz, 2H), 4.79 (d, J = 4.0 Hz, 1H), 7.11 (dd, J = 7.5 Hz, J = 1.0 Hz, 1H), 7.14 (d, J = 7.5 Hz, 1H), 7.23 (dd, J = 7.5 Hz, J = 1.0 Hz, 1H), 7.29−7.33 (m, 2H), 7.36 (td, J = 7.5 Hz, J = 1.5 Hz, 1H), 7.43 (d, J = 7.5 Hz, 1H). ^{13}C NMR (125 MHz, DMSO-d_6) δ [ppm] 19.44, 33.13 (d, J = 20.3 Hz), 33.75 (br s), 34.41 (br s), 44.56 (br s), 65.41, 83.03 (d, J = 165.1 Hz), 123.77, 126.46, 127.56, 128.06, 129.19, 129.42, 134.34 (d, J = 6.4 Hz), 135.38, 135.54, 140.50, 141.29, 168.67. LC/MS retention time: 7.96 min. MS (ESI) m/z = 342.2 $[M + H]^+$.

*Synthesis of **14**. 4-[2′-(2-Fluoroethyl)-2-methylbiphenyl-4-carbonyl]-piperazine-1-carboxylic Acid tert-Butyl Ester (**25**; Intermediate of Reaction Step (a) in Scheme 2).* The compound was synthesized using 258 mg (1.0 mmol) of **9** and 230 mg (1.2 mmol) of *N*-Boc-piperazine according to the procedure for the synthesis of **6b**. The obtained crude product was purified by column chromatography (*n*-hexane:EtOAc = 3:2) to yield 414 mg (97%) of the titled product as a white solid; mp 55−58 °C. ^{1}H NMR (500 MHz, DMSO-d_6) δ [ppm]: 1.42 (s, 9H), 2.01 (s, 3H), 2.59−2.69 (m, 1H), 2.75−2.86 (m, 1H), 3.40 (br s, 6H), 3.57 (br s, 2H), 4.45 (dt, J = 47.0 Hz, J = 6.5 Hz, 2H), 7.10 (dd, J = 7.5 Hz, J = 1.5 Hz, 1H), 7.16 (d, J = 7.5 Hz, 1H), 7.28 (dd, J = 7.5 Hz, J = 1.5 Hz, 1H), 7.32 (td, J = 7.5 Hz, J = 1.5 Hz, 1H), 7.35−7.38 (m, 2H), 7.44 (d, J = 7.5 Hz, 1H).

*[2′-(2-Fluoroethyl)-2-methylbiphenyl-4-yl]-piperazin-1-yl-methanone (**11**).* To a stirred solution of 900 mg (2.1 mmol) of **25** in 50 mL of CH_2Cl_2 under argon atmosphere, 5 mL (65 mmol) of trifluoroacetic acid was added After stirring for 2.5 h at rt, the complete consumption of **25** was confirmed by TLC analysis (*n*-hexane:EtOAc = 1:1) and the mixture was diluted with a saturated aqueous $NaHCO_3$ solution. The aqueous layer was extracted several times with EtOAc, and the resultant organic layer washed with brine and dried over Na_2SO_4. After filtration, the solvent was removed under reduced pressure and the

DOI: 10.1021/acs.jmedchem.5b01080
J. Med. Chem. XXXX, XXX, XXX−XXX

residue was treated with diethyl ether. The precipitate was filtered and dried in vacuum to give 700 mg (99%) of **11** as a white solid. ^{1}H NMR (500 MHz, DMSO-d_6) δ [ppm]: 2.01 (s, 3H), 2.58−2.69 (m, 1H), 2.75−2.85 (m, 4H), 3.20−3.70 (m, 6H), 4.45 (dt, J = 47.0 Hz, J = 6.5 Hz, 2H), 7.10 (dd, J = 7.5 Hz, J = 1.5 Hz, 1H), 7.15 (d, J = 7.5 Hz, 1H), 7.23−7.27 (m, 1H), 7.30−7.38 (m, 3H), 7.44 (d, J = 7.5 Hz, 1H).

*[2′-(2-Fluoroethyl)-2-methylbiphenyl-4-yl]-[4-(2-hydroxyethyl)-piperazin-1-yl]methanone (**14**).* To a stirred solution of 300 mg (0.9 mmol) of **11** in 7.5 mL of acetonitrile, 1.2 g (8.7 mmol) potassium carbonate and 0.1 mL (1.5 mmol) of 2-bromoethanol were added. After heating under reflux overnight, the consumption of the reactants was observed by TLC analysis (CH_2Cl_2:methanol = 9:1) and additional 0.05 mL (0.75 mmol) of 2-bromoethanol were added. After further refluxing for 4 h, the solvent was removed in vacuum and the residue was diluted with EtOAc. The resultant organic layer was washed with H_2O, dried over Na_2SO_4, filtered, and concentrated in vacuum. The crude product was purified by column chromatography (CH_2Cl_2:methanol = 95:5) to yield 200 mg (59%) of **14** as a white foam; mp 55−60 °C. ^{1}H NMR (500 MHz, DMSO-d_6) δ [ppm]: 2.01 (s, 3H), 2.43 (t, J = 6.0 Hz, 1H), 2.44 (br s, 5H), 2.58−2.69 (m, 1H), 2.75−2.85 (m, 1H), 3.40 (br s, 2H), 3.53 (q, J = 6.0 Hz, 2H), 3.62 (br s, 2H), 4.38−4.43 (m, 2H), 4.50 (t, J = 6.5 Hz, 1H), 7.11 (dd, J = 7.5 Hz, J = 1.0 Hz, 1H), 7.15 (d, J = 7.5 Hz, 1H), 7.24 (dd, 7.5 Hz, J = 1.5 Hz, 1H), 7.30−7.34 (m, 2H), 7.36 (td, J = 7.5 Hz, J = 1.5 Hz, 1H), 7.44 (d, J = 7.5 Hz, 1H). ^{13}C NMR (125 MHz, DMSO-d_6) δ [ppm]: 19.59, 33.17 (d, J = 20.3 Hz), 47.04, 52.99, 58.21, 59.81, 82.72 (d, J = 164.0 Hz), 123.42, 125.83, 126.94, 127.66, 128.55, 128.55, 128.78, 133.65 (d, J = 6.3 Hz), 134.26, 134.89, 139.73, 140.70, 167.71. LC/MS retention time: 6.72 min. MS (ESI) m/z = 371.2 $[M + H]^+$.

4.2. In Vitro Binding Studies. The studies were performed using membrane homogenates prepared from CHO cells stably transfected with human oxytocin receptor gene (hOTR-CHO; obtained from Bice Chini, Instituto di Neuroscienze, Consiglio Nazionale delle Ricerche, Milano, Italy). For the competitive binding studies, membrane preparation was incubated with [^{3}H]oxytocin (K_D = 2.56 nM ± 0.95 nM; [tyrosyl-2,6-^{3}H],1676 GBq/mmol; PerkinElmer LAS GmbH, Rodgau, Germany) at 1 nM and seven concentrations of test compounds (10 pM to 10 μM) in buffer consisting of 50 mM TRIS-HCl, pH 7.4, 5 mM $MgCl_2$, and 0.1% BSA for 60 min at 22 °C. The binding was terminated by rapid filtration (48-well semiautomated cell harvester; Brandel, Gaithersburg, USA) using GF/B glass fiber filter presoaked in 0.3% PEI for 60 min at rt. Radioactivity trapped on the filters was counted by liquid scintillation counting (Beckman LSC 6500; Beckman Coulter GmbH, Krefeld, Germany). Nonspecific binding was defined as binding remaining in the presence of 10 μM oxytocin. The assays were performed two times, each in duplicate. Experimental data were analyzed by nonlinear regression, and IC_{50} curves generated by a one-site competition model. The K_i values of the test compounds were calculated using the Cheng−Prusoff equation.

The equilibrium dissociation constant K_D of **6b** was determined performing a homologous binding experiment. [^{18}F]**6b** (specific activity: 160 GBq/μmol) at a radioactivity concentration of 57 kBq/mL (identical to a chemical concentration of 0.35 nM) was coincubated with various dilutions of **6b** (final concentration 0.1 nM−100 μM) with membranes obtained from hOTR-CHO cells in buffer consisting of 50 mM TRIS-HCl, pH 7.4, 5 mM $MgCl_2$, and 0.1% BSA for 60 min at 22 °C. The binding was terminated by rapid filtration (48-well semiautomated cell harvester; Brandel, Gaithersburg, USA) using GF/B glass fiber filter presoaked in 0.3% PEI for 60 min at rt. Radioactivity trapped on the filters was counted by gamma-counting (Wallac 1470 Wizard 3″; PerkinElmer LAS GmbH, Rodgau, Germany). CPM data were analyzed by nonlinear regression, and an IC_{50} curve generated by a one-site competition model. The K_D value of **6b** was calculated according to $K_D = IC_{50} - [\text{radioligand}]$, valid for the one-site homologous competition binding model.

4.3. Determination of log *D* and P_m Values. The log *D* values were determined by HPLC (Agilent 1100/1200 series) according to Donovan and Pescatore.[33] The compounds were injected (2 μL, 150 μg/mL) together with a mixture of toluene (0.5 mL) and triphenylene (5 mg) as internal standards in methanol (50 mL) to a short polymeric ODP-50 column (20 mm × 4 mm, 5 μm, Shodex, Showa Denko Europe GmbH, Munich, Germany) using a linear gradient from 10% methanol and 90% 10 mM sodium phosphate buffer to 100% methanol within 9.4 min at a flow rate of 1.5 mL/min and a pH of 7.4.

Permeability (P_m) measurements were performed according to Taillardat-Bertschinger et al. using immobilized artificial membrane (IAM) chromatography.[34,42] For IAM measurements, the same HPLC system and an IAM.PC.DD2 (150 mm × 4.6 mm, Regis Technologies Inc., Morton Grove, USA) column were used isocratically with 10 mM phosphate buffer and acetonitrile in different ratios (50/50, 55/45, 60/40, and 65/35) adjusted to pH 7.0 and 1 mL/min flow rate. P_m values are obtained by dividing membrane partition coefficient K_m by the molecular weight of the tracer candidates. K_m was calculated on the basis of the capacity factors k_{IAM} and correction of the column conditions (total volume of solvent within column (V_m) and volume of interphase (V_s)), at which the k_{IAM} factors are calculated and extrapolated to 100% aqueous phase.

4.4. Determination of Plasma-Free Fraction. Binding of [^{18}F]**6b** to plasma proteins was estimated by ultrafiltration. First, 1 mL of plasma obtained from pig was spiked with 60 μL of saline containing 10 MBq [^{18}F]**6b** and incubated for 30 min at 37 °C. The separation of protein-bound and free [^{18}F]**6b** was achieved by filtration through anisotropic hydrophilic Ultracel YM membrane (Amicon Centrifree, 30000 MW cutoff; MerckMilliporeAmicon Inc., USA) as specified by the manufacturer (2000*g*, 15 min, 21 °C). The radioactivity concentrations in the plasma obtained before centrifugation (C) and of the ultrafiltrate (C_u) were estimated by gamma counting of respective sample aliquots (Wallac 1470 Wizard 3″; PerkinElmer LAS GmbH, Rodgau, Germany). The value of plasma free fraction f_P was calculated according to the relation f_P (%) = C_u /C × 100.

4.5. Radiochemistry. No-carrier-added [^{18}F]fluoride was produced via the [^{18}O(p,n)^{18}F] nuclear reaction by irradiation of an [^{18}O]H_2O target (Hyox 18 enriched water, Rotem Industries Ltd., Israel) on a Cyclone 18/9 (iba RadioPharma Solutions, Belgium) with fixed energy proton beam using a Nirta [^{18}F]fluoride XL target. Microwave assisted radiofluorination was performed in a standard 4 mL V vial using a Discover PETWave Microwave (CEM, NC, USA).

Radio thin-layer chromatography (radio-TLC) was performed on silica gel (Polygram SIL G/UV_{254}) and aluminum oxide (Polygram Alox N/UV_{254}) precoated plates with EtOAc (EE)/PE (PE) 5/1 (for labeling product) and EE/EtOH 10/1 (for [^{18}F]**2**), respectively. The plates were exposed to storage phosphor screens (BAS-TR2025, FUJIFILM Co., Tokyo, Japan) and recorded using a bioimaging analyzer system (BAS-1800 II, FUJIFILM). Images were evaluated with the BASReader and AIDA 2.31 software (raytest Isotopenmessgeräte GmbH, Straubenhardt, Germany).

Analytical chromatographic separations were performed on a JASCO LC-2000 system, incorporating a PU-2080Plus pump, AS-2055Plus auto injector (100 μL sample loop), and a UV-2070Plus detector coupled with a gamma radioactivity HPLC detector (Gabi Star, raytest Isotopenmessgeräte GmbH). Data analysis was performed with the Galaxie chromatography software (Agilent Technologies) using the chromatograms obtained at 254 and 272 nm, respectively.

Semipreparative HPLC separations were performed on a JASCO LC-2000 system, incorporating a PU-2080-20 pump, a UV/vis-2075 detector coupled with a gamma radioactivity HPLC detector whose measurement geometry was slightly modified (Gabi Star, raytest Isotopenmessgeräte GmbH), and a fraction collector (Advantec CHF-122SC). Data analysis was performed with the Galaxie chromatography software (Agilent Technologies) using the chromatograms obtained at 254 nm.

The ammonium acetate (NH_4OAc) concentration stated as 20 mM NH_4OAc aq corresponds to the concentration in the aqueous component of an eluent mixture.

Radiosyntheses. No-carrier-added [^{18}F]fluoride in 2 mL of H_2O was trapped on a Chromafix 30 PS-HCO_3^- cartridge (Macherey-Nagel GmbH & Co. KG, Düren, Germany). The activity was eluted with 300 μL of an aqueous solution of potassium carbonate (K_2CO_3, 1.8 mg, 13

DOI: 10.1021/acs.jmedchem.5b01080
J. Med. Chem. XXXX, XXX, XXX−XXX

μmol) into a 4 mL V vial and Kryptofix 2.2.2 ($K_{2.2.2}$, 11 mg, 29 μmol) in 1 mL of ACN was added. The aqueous [^{18}F]fluoride was azeotropically dried under vacuum and nitrogen flow within 7−10 min using a single mode microwave (75 W, at 50−60 °C, power cycling mode). Two aliquots of ACN (2 × 1.0 mL) were added during the drying procedure, and the final complex was dissolved in 1000 μL of ACN ready for labeling. The reactivity of the anhydrous K[^{18}F]F-$K_{2.2.2}$-carbonate complex as well as the reproducibility of the drying procedure were checked via the standard reaction with 2 mg (5.4 μmol) of ethylene glycol ditosylate (Sigma-Aldrich, Germany) at 80 °C for 10 min in ACN. Thereafter, a solution of 2.0−2.5 mg of precursor in 500 μL of ACN was added and the ^{18}F-labeling was performed under thermal heating (90 °C, 15 min) or microwave-assisted irradiation (75W, 85−95 °C, 9 min, power cycling mode). To analyze the reaction mixture and to determine labeling yields, samples were taken for radio-HPLC and radio-TLC. Moreover, the stability of the tosylate precursor was investigated under both heating conditions used by HPLC analysis at different time points of the reaction.

After cooling to <30 °C, hydrochloric acid was added and the deprotection was performed by thermal heating (90 °C, 15 min, 1 mL 2.0 M HCl) or microwave irradiation (50W, 75−85 °C, 5 min, power cycling mode, 1 mL 2.0 M HCl). Thereafter, the reaction mixture was neutralized with aqueous 6.0 M NaOH and directly applied to an isocratic semipreparative RP-HPLC for isolation of [^{18}F]**6b** (44% ACN/20 mM NH_4OAc_{aq}, 4 mL/min, Reprosil-Pur C18-AQ, 250 mm × 10 mm; 5 μm; Dr. Maisch HPLC GmbH, Germany). The collected radiotracer fraction was diluted with 40 mL of H_2O to perform final purification by sorption on a Sep-Pak C18 light cartridge (Waters, Milford, MA, USA) and successive elution with 0.75 mL of ethanol. The solvent was reduced under a gentle argon stream and the desired radiotracer formulated in sterile isotonic saline containing 10% EtOH (v/v). The identity and radiochemical purity of [^{18}F]**6b** was confirmed by radio-HPLC (gradient and isocratic mode) and radio-TLC (Alox N/UV_{254}, EE/EtOH 10/1). For radio-HPLC, a Reprosil-Pur C18-AQ column (250 mm × 4.6 mm; 5 μm; Dr. Maisch HPLC GmbH; Germany) with ACN/20 mM NH_4OAc aq as eluent mixture and a flow of 1.0 mL/min was used (gradient: eluent A 10% ACN/20 mM NH_4OAc aq; eluent B 90% ACN/20 mM NH_4OAc aq; 0−5 min 100% A, 5−10 min up to 55% B, 10−25 min 55% B, 25−30 up to 100% B, 30−40 min 100% B, 40−45 min up to 100% A, and 45−55 min 100% A; isocratic, 42% ACN/20 mM NH_4OAc_{aq}). Specific activity was determined on the base of a calibration curve carried out under isocratic HPLC conditions (42% ACN/20 mM NH_4OAc_{aq}) using chromatograms obtained at 272 nm as an appropriate maximum of UV absorbance.

In Vitro Stability and Partition Coefficient. The in vitro stability of [^{18}F]**6b** was investigated by incubation of small tracer amounts (10−15 MBq) at 40 °C in 1 mL of following solutions: (i) 0.9% aq NaCl, (ii) PBS (137 mM NaCl, 2.7 mM KCl, 10 mM Na_2HPO_4; pH = 7.4), and (iii) pig plasma samples. At various time points, aliquots were analyzed by radio-TLC and radio-HPLC.

The partition coefficient of [^{18}F]**6b** was experimentally determined for the *n*-octanol/PBS system by the shake-flask method. Aliquots of the formulated radiotracer product were diluted in the buffer (20−50 μL, 1:1000) and added to a mixture of 3.0 mL of pre-equilibrated *n*-octanol and 3.0 mL of PBS. After shaking for 20 min at room temperature, the samples were centrifuged (5000*g*, 5 min), and duplicates of samples (0.5 mL each) of the organic as well as the aqueous layers were measured in a gamma counter. Another duplicate of samples (1 mL each) of the organic layer was subjected to the same procedure until constant partition coefficient values had been obtained. All measurements were done in triplicate.

*Radiotracer Metabolism of [^{18}F]**6b** in Mice.* Blood samples of mouse were taken at 30 min after intravenous injection of 84 MBq of [^{18}F]**6b** (n = 2). Pig blood samples were taken at 2, 8, 30, and 60 min after intravenous injection of 250 MBq of [^{18}F]**6b**. Plasma was obtained by centrifugation of blood at 12000 rpm at 4 °C for 10 min. Protein precipitation was performed by addition of ice-cold ACN in a ratio of 4:1 of organic solvent to plasma. The samples were vortexed for 2 min, equilibrated on ice for 15 min, and centrifuged for 5 min at 10000 rpm. The precipitates were washed with 200 μL of solvent mixture and subjected to the same procedure. The combined supernatants (total volume between 1.0−1.5 mL) were concentrated at 65 °C under argon flow to a final volume of approximately 100 μL and analyzed by radio-TLC and analytical radio-HPLC. To determine the percentage of radioactivity in the supernatants compared to total activity, aliquots of each step as well as the precipitates were quantified by gamma counting.

4.6. In Vitro Autoradiographic Studies. Brain sections (20 μm) of flash-frozen brains of female domestic pigs (*Sus s. domestica*, 6 weeks, 12−14 kg) were cut using a cryostat, thaw-mounted onto microscope slides, and after air-drying stored at −80 °C until use. Briefly, the brain sections were allowed to thaw in air and rinsed twice in 50 mM Tris buffer, pH 7.4, to remove endogenous ligand. The sections were then incubated with the 6 nM [^{3}H]oxytocin [tyrosyl-2,6-^{3}H], 1676 GBq/mmol; PerkinElmer LAS GmbH, Rodgau, Germany) or ∼10 nM [^{18}F]**6b** in TRIS buffer (50 mM TRIS-HCl, 5 mM NaCl, 0.1% BSA pH 7.4) for 60 min at room temperature. Nonspecific binding was determined in the presence of 10 or 0.1 μM oxytocin, respectively. Displacement of [^{18}F]**6b** was also evaluated with the following ligands: 1 μM L-quisqualic acid (glutamate receptor ligand), 0.35 μM THIP ($GABA_A$ receptor ligand), 0.2 μM siramesin (σ1/2 receptor ligand), 0.08 nM SR49059 (V_{1A} receptor ligand), or 3 nM tolvaptan ($V_{1/2}$ receptor ligand). Subsequently, the sections were washed twice for 2 min in ice-cold TRIS buffer and rinsed for 5 s in ice-cold distilled H_2O. The sections were rapidly dried in a stream of cold air before being exposed to a tritium-sensitive imaging plate. Developed autoradiographs were analyzed in a phosphor imager (Fuji BAS 1800 II). The quantification was performed by using 2D-densitometric analysis (AIDA 2.31 software; raytest Isotopenmessgeräte GmbH, Germany).

4.7. In Vivo Studies in Mice. Animals for in vivo studies were obtained from the Medizinisch-Experimentelles Zentrum, Universität Leipzig. All procedures that include animals were approved by the respective State Animal Care and Use committee and conducted in accordance with the German Law for the Protection of Animals (TVV 08/13). For all in vivo studies in mice, female CD-1 mice, 10−12 weeks old, 20−25 g, were used.

*Biodistribution of [^{18}F]**6b** in Mice.* Mice received an injection of approximately 200 kBq [^{18}F]**6b** with a specific activity of 70 GBq/μmol in 200 μL of 0.9% saline into the tail vein. The animals were anesthetized for blood and urine sampling and euthanized by luxation of the cervical spine at 5 and 30 min pi (n = 2 per each time point). The organs of interest were removed and weighed, and the radioactivity was measured by gamma counting (Wallac 1470 Wizard 3″; PerkinElmer LAS GmbH, Rodgau, Germany). The percentage of injected dose per gram of wet tissue (% ID/g wet weight) was calculated.

*PET/MR Studies of [^{18}F]**6b** in Mice.* Mouse small animal PET acquisitions were obtained on a preclinical PET/MR system (nanoScan PET/MR, Mediso Medical Imaging Systems, Budapest, Hungary). Anesthesia was induced by exposing mice to 4% isoflurane in air and then maintained by reducing the ratio to 1.5% for the duration of the studies. The animal was placed in the PET scanner followed by a 15 min MR scan. The subsequent 60 min PET scan was started with the beginning of the intravenous injection of [^{18}F]**6b** (mean = 11.8 MBq; 10.4−13.1 MBq), and radioactivity concentration was measured in sequential frames of 5 min duration. Activity volumes were reconstructed with iterative reconstruction (OSEM, four iterations, six subsets) including an MR-based attenuation and scatter correction, achieving a reconstructed spatial resolution of 1.5 mm.[45] Additional experiments were similarly performed in mice preinjected with cyclosporin (50 mg/kg iv, 60 min prior to radioligand administration).

4.8. PET Study in Pig. Animal procedure was approved by the Animal Care and Use Committee of Saxony (TVV 08/13). One piglet (6 weeks old) was used in this study. Anaesthesia and surgery of the animal was performed as described previously.[56] In brief, the animal was premedicated with midazolam (1 mg·kg^{-1} im) followed by induction of anesthesia with 3% isoflurane in 70% N_2O/30% O_2. All

DOI: 10.1021/acs.jmedchem.5b01080
J. Med. Chem. XXXX, XXX, XXX−XXX

incision sites were infiltrated with 1% lidocaine, and anesthesia was maintained throughout the surgical procedure with 1.5% isoflurane. A central venous catheter was introduced through the left external jugular vein and used for the administration of the radiotracer and drugs and for volume substitution with heparinized (50 IE·mL^{-1}) lactated Ringer's solution (2 mL·kg^{-1}·h^{-1}). An endotracheal tube was inserted by tracheotomy for artificial ventilation (Servo Ventilator 900C, Siemens-Elema, Sweden) after immobilization with pancuronium bromide (0.2 mg·kg^{-1}·h^{-1}). The artificial ventilation was adjusted to maintain normoxia and normocapnia (Radiometer ABL 500, Copenhagen, Denmark). Polyurethane catheters (Ø 0.5 mm) were advanced through the left and the right femoral arteries into the abdominal aorta to withdraw arterial blood samples for regular monitoring of blood gases and for radiotracer input function measurements. Body temperature was monitored by a rectal temperature probe and maintained at ∼38 °C by a heating pad. After completion of surgery, anesthesia was maintained with 0.5% isoflurane in 70% N_2O/30% O_2, and the animal was allowed to stabilize for 1 h before PET imaging.

PET Scanning Protocol. PET imaging was performed according to the protocol described recently.[57] In brief, animals were scanned position prone, with the head held in the aperture of a clinical tomograph (ECAT EXACT HR+, CTI/Siemens) using a custom-made head holder. For attenuation and scatter correction, transmission scans were acquired using three rotating ^{68}Ge rod sources. [^{18}F]**6b** (225 MBq; A_s, 54 GBq/μmol) was applied in 10 mL saline as a 2 min iv infusion using a syringe pump, followed by flushing with 10 mL of heparinized saline (50 IE·mL^{-1}). The emission recording started upon initiation of the injection, and dynamic emission data were acquired for a total of 120 min. Arterial blood was sampled continuously using a peristaltic pump during the first 20 min of the recording, followed by manual sampling at 25, 30, 40, 50, 60, 90, and 120 min after injection. After centrifugation, the plasma radioactivity concentration was measured using a gamma counter (1470 Wizard, PerkinElmer, Shelton, CT, USA) cross calibrated to the PET scanner. Additionally, arterial blood was sampled manually at 4, 16, 30, and 60 min pi and plasma obtained as described above to determine the fractions of nonmetabolized [^{18}F]**6b** (see below).

Quantification of PET Data. After correction for attenuation, scatter, decay, and scanner-specific dead time, images were reconstructed by filtered back projection using a 4.9 mm FWHM Hanning filter into 40 frames of increasing length. A summed PET image of a 30 min FDG scan of the same pig, performed directly after the first PET scan, was used for alignment with a T1-weighed MR image of a 6-week-old farm-bred pig as described previously.[58] The following volumes of interest (VOIs) were chosen: olfactory bulb, frontal cortex, hippocampus, striatum (defined as mean radioactivity in caudate and putamen), colliculi, and cerebellum. Radioactivity in all VOIs was calculated as the mean radioactivity concentration (Bq/mL) for the left and right sides. To generate standardized uptake values (SUVs) the VOI activities were normalized to the injected dose and corrected for animal weight.

AUTHOR INFORMATION

Corresponding Author

*E-mail: b.wenzel@hzdr.de. Phone: +49 341 2341794637.

Author Contributions

#B.W. and J.M. contributed equally to this work.

Notes

The authors declare no competing financial interest.

ACKNOWLEDGMENTS

The project was funded by Europäischer Fonds für regionale Entwicklung (EFRE). We thank Dr. Karsten Franke for providing [^{18}F]fluoride. We thank Dr. Achim Hiller, Juliane Schaller, and Tina Spalholz for their assistance in the lab. We are very grateful to Bice Chini from the Instituto di Neuroscienze, Milano, Italy, for providing the hOTR-CHO cell line.

ABBREVIATIONS USED

ACN, acetonitrile; EtOAc, ethyl acetate; PE, petroleum ether; Hünig's base, *N*,*N*-diisopropylamine; Steglich base, 4-dimethylaminopyridine; COMU, (1-cyano-2-ethoxy-2-oxoethylidenaminooxy)dimethylamino-morpholino-carbenium hexafluorophosphate; TBTU, *O*-(benzotriazol-1-yl)-*N*,*N*,*N*′,*N*′-tetramethyluronium tetrafluoroborate; HATU, 1-bis-(dimethylamino)methylene-1*H*-1,2,3-triazolo[4,5-*b*]-pyridinium-3-oxid hexafluorophosphate; EDCI, 1-ethyl-3-(3-dimethylamino-propyl) carbodiimide hydrochloride carbodiimide hydrochloride; HOBt, 1-hydroxybenzotriazole; DAST, diethylaminosulfur trifluoride; TAC, time−activity curve; VOI, volume of interest; SUV, standard uptake value; V_T, distribution volume; BP, binding potential; PSA, polar surface area; TPSA, topological polar surface area

REFERENCES

(1) Nussey, S.; Whitehead, S. The pituitary gland. In *Endocrinology: An Integrated Approach*; BIOS Scientific Publisher: Oxford, 2001; Chapter 7.

(2) Gimpl, G.; Fahrenholz, F. The oxytocin receptor system: structure, function, and regulation. *Physiol. Rev.* **2001**, *81*, 629−683.

(3) Viero, C.; Shibuya, I.; Kitamura, N.; Verkhratsky, A.; Fujihara, H.; Katoh, A.; Ueta, Y.; Zingg, H. H.; Chvatal, A.; Sykova, E.; Dayanithi, G. REVIEW: Oxytocin: Crossing the bridge between basic science and pharmacotherapy. *CNS Neurosci. Ther.* **2010**, *16*, e138−56.

(4) Loup, F.; Tribollet, E.; Dubois-Dauphin, M.; Dreifuss, J. J. Localization of high-affinity binding sites for oxytocin and vasopressin in the human brain. An autoradiographic study. *Brain Res.* **1991**, *555*, 220−32.

(5) Freeman, S. M.; Inoue, K.; Smith, A. L.; Goodman, M. M.; Young, L. J. The neuroanatomical distribution of oxytocin receptor binding and mRNA in the male rhesus macaque (Macaca mulatta). *Psychoneuroendocrinology* **2014**, *45*, 128−41.

(6) Tribollet, E.; Audigier, S.; Dubois-Dauphin, M.; Dreifuss, J. J. Gonadal steroids regulate oxytocin receptors but not vasopressin receptors in the brain of male and female rats. An autoradiographical study. *Brain Res.* **1990**, *511*, 129−40.

(7) Freund-Mercier, M. J.; Stoeckel, M. E.; Palacios, J. M.; Pazos, A.; Reichhart, J. M.; Porte, A.; Richard, P. Pharmacological characteristics and anatomical distribution of [^{3}H]oxytocin-binding sites in the Wistar rat brain studied by autoradiography. *Neuroscience* **1987**, *20*, 599−614.

(8) Freund-Mercier, M. J.; Stoeckel, M. E.; Waeber, C.; Kremarik, P.; Palacios, J. M.; Richard, P. Neurophysins, rather than Receptors, are Involved in [^{3}H]Oxytocin and [^{3}H]Vasopressin Binding Detected by Autoradiography in the Hypothalamo-Neurohypophyseal System. *J. Neuroendocrinol.* **1991**, *3*, 285−95.

(9) Neumann, I. D. Brain oxytocin: a key regulator of emotional and social behaviours in both females and males. *J. Neuroendocrinol.* **2008**, *20*, 858−65.

(10) Ross, H. E.; Young, L. J. Oxytocin and the neural mechanisms regulating social cognition and affiliative behavior. *Front. Neuroendocrinol.* **2009**, *30*, 534−47.

(11) Insel, T. R.; Young, L. J. The neurobiology of attachment. *Nat. Rev. Neurosci.* **2001**, *2*, 129−36.

(12) Macdonald, K.; Macdonald, T. M. The peptide that binds: a systematic review of oxytocin and its prosocial effects in humans. *Harv. Rev. Psychiatry* **2010**, *18*, 1−21.

(13) Zink, C. F.; Meyer-Lindenberg, A. Human neuroimaging of oxytocin and vasopressin in social cognition. *Horm. Behav.* **2012**, *61*, 400−9.

(14) Meyer-Lindenberg, A.; Domes, G.; Kirsch, P.; Heinrichs, M. Oxytocin and vasopressin in the human brain: social neuropeptides for translational medicine. *Nat. Rev. Neurosci.* **2011**, *12*, 524−38.

DOI: 10.1021/acs.jmedchem.5b01080
J. Med. Chem. XXXX, XXX, XXX−XXX

(15) Kanat, M.; Heinrichs, M.; Domes, G. Oxytocin and the social brain: Neural mechanisms and perspectives in human research. *Brain Res.* **2014**, *1580*, 160−171.
(16) Neumann, I. D. The advantage of social living: brain neuropeptides mediate the beneficial consequences of sex and motherhood. *Front. Neuroendocrinol.* **2009**, *30*, 483−96.
(17) Goldman, M.; Marlow-O'Connor, M.; Torres, I.; Carter, C. S. Diminished plasma oxytocin in schizophrenic patients with neuroendocrine dysfunction and emotional deficits. *Schizophr. Res.* **2008**, *98*, 247−55.
(18) MacDonald, K.; MacDonald, T. M.; Brune, M.; Lamb, K.; Wilson, M. P.; Golshan, S.; Feifel, D. Oxytocin and psychotherapy: a pilot study of its physiological, behavioral and subjective effects in males with depression. *Psychoneuroendocrinology* **2013**, *38*, 2831−43.
(19) Green, J. J.; Hollander, E. Autism and oxytocin: new developments in translational approaches to therapeutics. *Neurotherapeutics* **2010**, *7*, 250−7.
(20) Green, L.; Fein, D.; Modahl, C.; Feinstein, C.; Waterhouse, L.; Morris, M. Oxytocin and autistic disorder: alterations in peptide forms. *Biol. Psychiatry* **2001**, *50*, 609−13.
(21) Smith, A. L.; Freeman, S. M.; Stehouwer, J. S.; Inoue, K.; Voll, R. J.; Young, L. J.; Goodman, M. M. Synthesis and evaluation of C-11, F-18 and I-125 small molecule radioligands for detecting oxytocin receptors. *Bioorg. Med. Chem.* **2012**, *20*, 2721−38.
(22) Smith, A. L.; Freeman, S. M.; Voll, R. J.; Young, L. J.; Goodman, M. M. Investigation of an F-18 oxytocin receptor selective ligand via PET imaging. *Bioorg. Med. Chem. Lett.* **2013**, *23*, 5415−20.
(23) Smith, A. L.; Freeman, S. M.; Voll, R. J.; Young, L. J.; Goodman, M. M. Carbon-11 N-methyl alkylation of L-368,899 and in vivo PET imaging investigations for neural oxytocin receptors. *Bioorg. Med. Chem. Lett.* **2013**, *23*, 902−6.
(24) Lemaire, W.; O'Brien, J. A.; Burno, M.; Chaudhary, A. G.; Dean, D. C.; Williams, P. D.; Freidinger, R. M.; Pettibone, D. J.; Williams, D. L., Jr. A nonpeptide oxytocin receptor antagonist radioligand highly selective for human receptors. *Eur. J. Pharmacol.* **2002**, *450*, 19−28.
(25) Williams, P. D.; Anderson, P. S.; Ball, R. G.; Bock, M. G.; Carroll, L.; Chiu, S. H. L.; Clineschmidt, B. V.; Culberson, J. C.; Erb, J. M.; Evans, B. E.; Fitzpatrick, S. L.; Freidinger, R. M.; Kaufman, M. J.; Lundell, G. F.; Murphy, J. S.; Pawluczyk, J. M.; Perlow, D. S.; Pettibone, D. J.; Pitzenberg, S. M.; Thompson, K. L.; Veber, D. F.; et al. 1-((7,7-Dimethyl-2(S)-(2(S)-amino-4-(methylsulfonyl)-butyramido)bicyclo [2.2.1]-heptan-1(S)-yl)methyl)sulfonyl)-4-(2-methylphenyl)piperaz ine (L-368,899): an orally bioavailable, non-peptide oxytocin antagonist with potential utility for managing preterm labor. *J. Med. Chem.* **1994**, *37*, 565−571.
(26) Failli, A. A.; Shumsky, J. S.; Caggiano, T. J.; Sabatucci, P. J.; Memoli, K. A.; Trybulski, E. J.; Sanders, W. J. Novel tricyclic hydroxy carboxamides and derivatives thereof tocolytic oxytocin receptor antagonists. (Wyeth) WO 02/083680, 2002.
(27) Ring, R. H.; Malberg, J. E.; Potestio, L.; Ping, J.; Boikess, S.; Luo, B.; Schechter, L. E.; Rizzo, S.; Rahman, Z.; Rosenzweig-Lipson, S. Anxiolytic-like activity of oxytocin in male mice: behavioral and autonomic evidence, therapeutic implications. *Psychopharmacology* **2006**, *185*, 218−25.
(28) Chen, X.; Liu, Y.; Liu, D. K.; Wang, P. B. 1-(2-Nitrobenzyl)-1H-pyrrole-2-carbaldehyde. *Acta Crystallogr., Sect. E: Struct. Rep. Online* **2011**, *67*, O1473.
(29) Artico, M.; DeMartino, G.; Filacchioni, G.; Giuliano, R. Studies on substances with antitumor activity. XXXVI. Anthramycin and similar compounds. I. Synthesis of 10,11-diidro-5*H*-pyrrole-(2,1-*c*)(1,4)-benzodiazepine. *Farmaco Sci.* **1969**, *24*, 276−284.
(30) Wright, W. B.; Greenblatt, E. N.; Day, I. P.; Quinones, N. Q.; Hardy, R. A. Derivatives of 11-(1-Piperazinyl)-5h-Pyrrolo[2,1-C]-[1,4]Benzodiazepine as Central Nervous-System Agents. *J. Med. Chem.* **1980**, *23*, 462−465.
(31) Tang, P. C.; Li, X.; Li, X.; Chen, Y.; Wang, B.; Zhu, Z. Phtalazinone ketone derivative, preparation method thereof and pharmaceutical use thereof. (Jiangsu Hansoh Pharmaceutical Co., Ltd.) US 2013/0131068 A1, 2013.
(32) Cheng, Y.; Prusoff, W. H. Relationship between the inhibition constant (K1) and the concentration of inhibitor which causes 50% inhibition (I50) of an enzymatic reaction. *Biochem. Pharmacol.* **1973**, *22*, 3099−3108.
(33) Donovan, S. F.; Pescatore, M. C. Method for measuring the logarithm of the octanol-water partition coefficient by using short octadecyl-poly(vinyl alcohol) high-performance liquid chromatography columns. *J. Chromatogr. A* **2002**, *952*, 47−61.
(34) Taillardat-Bertschinger, A.; Carrupt, P. A.; Barbato, F.; Testa, B. Immobilized artificial membrane HPLC in drug research. *J. Med. Chem.* **2003**, *46*, 655−665.
(35) Waterhouse, R. N. Determination of lipophilicity and its use as a predictor of blood-brain barrier penetration of molecular imaging agents. *Mol. Imaging Biol.* **2003**, *5*, 376−89.
(36) Rankovic, Z. CNS drug design: balancing physicochemical properties for optimal brain exposure. *J. Med. Chem.* **2015**, *58*, 2584−608.
(37) van de Waterbeemd, H.; Camenisch, G.; Folkers, G.; Chretien, J. R.; Raevsky, O. A. Estimation of blood-brain barrier crossing of drugs using molecular size and shape, and H-bonding descriptors. *J. Drug Target.* **1998**, *6*, 151−65.
(38) Wils, P.; Warnery, A.; Phung-Ba, V.; Legrain, S.; Scherman, D. High lipophilicity decreases drug transport across intestinal epithelial cells. *J. Pharmacol. Exp. Ther.* **1994**, *269*, 654−658.
(39) Vallabhajosula, S. Radiolabeled Molecular Imaging Probe. In *Molecular Imaging: Radiopharmaceuticals for PET and SPECT*; Springer-Verlag: Dordrecht, Heidelberg, New York, 2009; p 141.
(40) Brust, P.; van den Hoff, J.; Steinbach, J. Development of ^{18}F-labeled radiotracers for neuroreceptor imaging with Positron Emission Tomography. *Neurosci. Bull.* **2014**, *30*, 777−811.
(41) Tavares, A. A.; Lewsey, J.; Dewar, D.; Pimlott, S. L. Radiotracer properties determined by high performance liquid chromatography: a potential tool for brain radiotracer discovery. *Nucl. Med. Biol.* **2012**, *39*, 127−35.
(42) Taillardat-Bertschinger, A.; Galland, A.; Carrupt, P. A.; Testa, B. Immobilized artificial membrane liquid chromatography: proposed guidelines for technical optimization of retention measurements. *J. Chromatogr. A* **2002**, *953*, 39−53.
(43) Vraka, C.; Nics, L.; Weiss, V.; Wagner, K.; Hacker, M.; Wadsak, W.; Mitterhauser, M. Combination of high throughput HPLC methods for rapid prediction of blood−brain barrier penetration of newly developed radiotracers. *Eur. J. Nucl. Med. Mol. Imaging* **2014**, *41*, S442.
(44) Freeman, S. M.; Walum, H.; Inoue, K.; Smith, A. L.; Goodman, M. M.; Bales, K. L.; Young, L. J. Neuroanatomical distribution of oxytocin and vasopressin 1a receptors in the socially monogamous coppery titi monkey (Callicebus cupreus). *Neuroscience* **2014**, *273*, 12−23.
(45) Kaur, N. An insight into medicinal and biological significance of privileged scaffold: 1,4-benzodiazepine. *Int. J. Pharm. Bio. Sci.* **2013**, *4*, 318−337.
(46) Freund-Mercier, M. J.; Stoeckel, M. E.; Dietl, M. M.; Palacios, J. M.; Richard, P. Quantitative autoradiographic mapping of neurohypophysial hormone binding sites in the rat forebrain and pituitary gland–I. Characterization of different types of binding sites and their distribution in the Long-Evans strain. *Neuroscience* **1988**, *26*, 261−72.
(47) Colaianni, G.; Tamma, R.; Di Benedetto, A.; Yuen, T.; Sun, L.; Zaidi, M.; Zallone, A. The oxytocin-bone axis. *J. Neuroendocrinol.* **2014**, *26*, 53−7.
(48) Demeule, M.; Wenger, R. M.; Beliveau, R. Molecular interactions of cyclosporin A with P-glycoprotein. Photolabeling with cyclosporin derivatives. *J. Biol. Chem.* **1997**, *272*, 6647−52.
(49) Syvänen, S.; Lindhe, O.; Palner, M.; Kornum, B. R.; Rahman, O.; Langstrom, B.; Knudsen, G. M.; Hammarlund-Udenaes, M. Species differences in blood-brain barrier transport of three positron emission tomography radioligands with emphasis on P-glycoprotein transport. *Drug Metab. Dispos.* **2009**, *37*, 635−43.
(50) Rötering, S.; Scheunemann, M.; Fischer, S.; Hiller, A.; Peters, D.; Deuther-Conrad, W.; Brust, P. Radiosynthesis and first evaluation

DOI: 10.1021/acs.jmedchem.5b01080
J. Med. Chem. XXXX, XXX, XXX−XXX

in mice of [^{18}F]NS14490 for molecular imaging of alpha7 nicotinic acetylcholine receptors. *Bioorg. Med. Chem.* **2013**, *21*, 2635−42.
(51) Rötering, S.; Deuther-Conrad, W.; Cumming, P.; Donat, C. K.; Scheunemann, M.; Fischer, S.; Xiong, G.; Steinbach, J.; Peters, D.; Sabri, O.; Bucerius, J.; Brust, P. Imaging of alpha7 nicotinic acetylcholine receptors in brain and cerebral vasculature of juvenile pigs with [^{18}F]NS14490. *EJNMMI Res.* **2014**, *4*, 43.
(52) Kelder, J.; Grootenhuis, P. D.; Bayada, D. M.; Delbressine, L. P.; Ploemen, J. P. Polar molecular surface as a dominating determinant for oral absorption and brain penetration of drugs. *Pharm. Res.* **1999**, *16*, 1514−9.
(53) TPSA calculation was performed by using the free Molecular Property Calculation service of Molinspiration (molinspiration.com).
(54) Ertl, P.; Rohde, B.; Selzer, P. Fast calculation of molecular polar surface area as a sum of fragment-based contributions and its application to the prediction of drug transport properties. *J. Med. Chem.* **2000**, *43*, 3714−7.
(55) Pajouhesh, H.; Lenz, G. R. Medicinal chemical properties of successful central nervous system drugs. *NeuroRx* **2005**, *2*, 541−53.
(56) Brust, P.; Patt, J. T.; Deuther-Conrad, W.; Becker, G.; Patt, M.; Schildan, A.; Sorger, D.; Kendziorra, K.; Meyer, P.; Steinbach, J.; Sabri, O. In vivo measurement of nicotinic acetylcholine receptors with [^{18}F]norchloro-fluoro-homoepibatidine. *Synapse* **2008**, *62*, 205−18.
(57) Deuther-Conrad, W.; Fischer, S.; Hiller, A.; Becker, G.; Cumming, P.; Xiong, G.; Funke, U.; Sabri, O.; Peters, D.; Brust, P. Assessment of alpha7 nicotinic acetylcholine receptor availability in juvenile pig brain with [^{18}F]NS10743. *Eur. J. Nucl. Med. Mol. Imaging* **2011**, *38*, 1541−9.
(58) Brust, P.; Zessin, J.; Kuwabara, H.; Pawelke, B.; Kretzschmar, M.; Hinz, R.; Bergman, J.; Eskola, O.; Solin, O.; Steinbach, J.; Johannsen, B. Positron emission tomography imaging of the serotonin transporter in the pig brain using [^{11}C](+)-McN5652 and S-([^{18}F]fluoromethyl)-(+)-McN5652. *Synapse* **2003**, *47*, 143−51.

DOI: 10.1021/acs.jmedchem.5b01080
J. Med. Chem. XXXX, XXX, XXX−XXX